
Fariza Metsana-Oussaid, Djelloul Belhai, Ignacio Arenillas, José Antonio Arz & Vicente Gilabert (2019): *New sections of the Cretaceous–Paleogene transition in the southwestern Tethys (Médéa, northern Algeria): planktic foraminiferal biostratigraphy and biochronology.* Arabian Journal of Geosciences (2019) 12:217.

DOI: 10.1007/s12517-019-4402-4.

Published online March 19, 2019

Avalaible in: https://link.springer.com/journal/12517

New sections of the Cretaceous-Paleogene transition in the southwestern Tethys (Médéa, northern Algeria): planktic foraminiferal biostratigraphy and biochronology

Fariza Metsana-Oussaid[1], Djelloul Belhai[1], Ignacio Arenillas[2,*], José Antonio Arz[2], Vicente Gilabert[2]

[1] Université des Sciences et de la Technologie Houari Boumediene (USTHB). Faculté des Sciences de la Terre, de Géographie et Aménagement du Territoire, Algérie.

[2] Departamento de Ciencias de la Tierra, and Instituto Universitario de Investigación en Ciencias Ambientales de Aragón (IUCA), Universidad de Zaragoza, E-50009, Spain.

[*] Corresponding author.

E-mail address: ias@unizar.es (I. Arenillas)

ORCID: 0000-0003-4632-533X (I. Arenillas)

Abstract Two sections (Sidi Ziane and Djebel Zakhamoune from Médéa, northern Algeria) of the Cretaceous-Paleogene (K-Pg) transition have been found, sampled and studied in detail for the first time in Algeria. In order to obtain a biochronological control to evaluate the potential of the Médéa area for the study of the K/Pg boundary event and close paleoclimatic episodes as LMWE and Dan-C2, we have reviewed the biostratigraphical scales with planktic foraminifera from the uppermost Maastrichtian to the middle Danian, and dated the main key-bioevents through graphic correlations comparing the Bottaccione (Italy), Agost and Caravaca (Spain), and Kalaat Senan (Tunisia) sections. The biostratigraphic study has revealed the presence of the last biozone of the Maastrichtian in both sections (Zone CF1 or *Plummerita hantkeninoides* Zone). The thickness of this biozone (13.5 m in Sidi Ziane and 9 m in Djebel Zakhamoune) is one of the largest identified to date, suggesting that the uppermost Maastrichtian is complete and continuous in the Médéa area. Based on graphic correlation, it has been determined that

sedimentation rates of the Maastrichtian in Sidi Ziane and Djebel Zakhamoune are respectively 8.98 and 6.58 cm/kyr, only comparable with the most expanded and continuous sections worldwide, such as Aïn Settara (Kalaat Senan). It has also recognized a hiatus affecting the lower Danian in both sections, estimated in 610.4 and 644.9 kyr long in Djebel Zakhamoune and Sidi Ziane respectively. Nevertheless, the presence of reworked specimens of the index-species *Parvularugoglobigerina longiapertura* strongly suggests that the lowermost Danian may be recorded in the Médéa area.

Keywords: Micropaleontology - Graphic correlation - Danian - Maastrichtian - Tell Atlas

Introduction

The 66 Ma mass extinction event at the Cretaceous/Paleogene (K/Pg) boundary is a well-known topic since Alvarez et al. (1980) at Gubbio (Italy) and Smit and Hertogen (1980) at Caravaca (Spain) proposed the hypothesis of asteroid impact as its trigger, and Hildebrand et al. (1991) found the impact crater in Chicxulub (Yucatan Peninsula, Mexico). Since then, numerous K/Pg boundary sections of pelagic environments have been identified, being the western Tethyan sections the first to be studied with high-resolution sampling (Smit 1982, 1999). In addition to the El Kef section (Tunisia), which was chose as Global boundary Stratotype Section and Point (GSSP) for the base of the Danian Stage or K/Pg boundary (Molina et al. 2006), other well-known western Tethyan sections are Bottaccione and Contessa/Contessa Highway in Gubbio (Italy), Agost and Caravaca (Spain), and Aïn Settara and Elles (Tunisia). The last three were chosen as auxiliary sections of the GSSP for the K/Pg boundary (Molina et al. 2009). However, there is a knowledge gap in Algeria, since no K-Pg transition section has yet been located and studied in detail. Identifying K/Pg boundary sections in Algeria would allow the study of the extinction event in the western Tethys to be completed.

In Algeria, there are two promising areas to identify K/Pg boundary sections in marine environments: Aurés Mountains and West-Central Tell Mountains, both the Atlas Mountain System. The Aurés Atlas area from Algeria may include sections and facies similar to those from Tunisia (belonging also to Aurés Mountains) where the most continuous, complete and expanded sections known to date have been identified, such as El Kef, Aïn Settara and Elles (Arz et al. 1999; Arenillas et al. 2000a, b;

Molina et al. 2009). However, the Tell Atlas is currently more interesting to explore and study since it belongs to a very unknown paleogeographic area in the K/Pg boundary study. It can provide new knowledge not only about the K/Pg boundary extinction event but also of the paleobiological, paleoenvironmental and paleoclimatic evolution during the late Maastrichtian and early Danian from the southwestern Tethys.

In addition to the K/Pg boundary extinction event, the Tellian domain could be important for the study of other close environmental and climatic episodes occurred during the K-Pg transition, as the "hyperthermal" warming episodes called Latest Maastrichtian Warming Event or LMWE (Barnet et al. 2017) and early Danian Dan-C2 (Quillévéré et al. 2008), which have been directly linked to the intensive volcanism of the Deccan Traps in the SE India (Chenet et al. 2007; Coccioni et al. 2010; Petersen et al. 2016; Thibault et al. 2016). The Tellian domain can also be useful to confirm or refute the hypotheses that the environmental and climatic changes linked to the main phase of Deccan volcanism played a key role in the end-Cretaceous extinctions (Keller 2003; Keller et al. 2011, 2016; Punekar et al. 2014, 2016; Font et al. 2016). Schoene et al. (2015) supported this hypothesis after concluding that the main Deccan phase occurred during the latest Maastrichtian. However, Renne et al. (2015) and Richards et al. (2015) suggested an alternative hypothesis according to which the main Deccan phase occurred in the early Danian and the Chicxulub impact could be its trigger.

After carrying out an intensive search of sections of the K-Pg transition in the Tellian domain, we came upon two promising sections: Sidi Ziane and Djebel Zakhamoune in the Médéa area (northern Algeria). In order to explore the potential of Algeria in the study of the K/Pg boundary event, we report here a high-resolution planktic foraminiferal biostratigraphic study of both sections. Based on graphic correlation with planktic foraminifera, we compare these sections with some of the most expanded and continuous sections in the western Tethys (Tunisia, Spain and Italy). Graphic correlation is a technique in which integrated stratigraphic key-data (mainly bio- and magnetostratigraphic data) are used to show correlation points between sections and geological time (Shaw 1964). The application of this technique has allowed us to establish a chronology of bioevents across the K/Pg boundary as well as inquire the degree of continuity of the Médéa sections and its potential to study the K/Pg boundary and close climatic episodes as the LMWE and Dan-C2.

Geographical and geological setting

The studied area is located in Souagui District of the Médéa Province (northern Algeria), which is approximately 75km south-west of Algiers and 47 km south-east of the city capital of Médéa (Fig. 1A). We have studied two sections, distant about 5 km, one to the east of the studied area, Sidi Ziane, and another to the west, Djebel Zakhamoune. They are localized in the southern half of the Souagui geological sheet (1/50.000) of Kieken in De Chevilly (1961). Both sections are located on the southern flank of Djebel Chaâba, characterized by fairly high reliefs with altitudes around 1200m. The Sidi Ziane section (3°15'12"E, 36°01'56"N) is placed 4 km south of the Sidi Ziane village, 10 km from the Souagui town, and 52 km from Médéa. The Sidi Ziane outcrops is easily accessible and well-exposed for the absence of vegetation. The Djebel Zakhamoune section (36°01'42"N, 3°12'05 E) is located 7 km east of the Rebaïa village, which is 10 km from Souagui, and 42 km south-east of Médéa.

The Souagui region is part of the Central Tellian Atlas (northern Algeria), and more precisely of the External Tell System or southern external domain of the Maghrebide chain (Auboin and Durand-Delga 1971), known for its complex tectonic evolution during the Mesozoic (Bouillin 1978; Guiraud et al. 2005). It also belongs to the eastern part of the Titteri range, a large area consisting of a superposition of several nappes of Cretaceous-Miocene age (Kieken 1963; Wildi 1983). This area is dominated in the northern part by autochthonous series, and in its southern part by allochthonous series of Cretaceous-Miocene age. According to De Chevilly (1961) and Kieken (1963, 1974), these formations are tectonized and differentiate into four tectonic units (IV, V, VI and VII). The VI unit has a significant extension in the central part of Souagui geological sheet, where the Cretaceous series are well developed, and it is subdivided into three subunits (VIa, VIb and VIc). Both Sidi Ziane and Djebel Zakhamoune sections are in the subunit VIa (Fig. 1B), in which outcrops materials of Maastrichtian-Oligocene age. In this subunit (Fig. 1C), the Danian stage was not distinguished from the Maastrichtian ones (De Chevilly 1961; Kieken 1963). They consist of black gray marls with gray calcareous marls.

The External Tell System was placed in the African paleo-margin of the southwestern Tethys. The External Tell sedimentary series were deposited in the southern part of the Tellian basin during the Mesozoic and Cenozoic. During the Maastrichtian, a large transgression was developed in the Tellian domain. It occurred as a consequence of the Campanian-Maastrichtian rifting phase after the Late Santonian -compressional- tectonic event described by Guiraud (1998) and Guiraud et al. (2005). Subsident basins of orientation approximately E-W, as the Tellian basin, were developed along the

northern African Tethyan margin (Wildi 1983). The high sea level was responsible for the deposition of thick marl-limestone series during the Maastrichtian of the Tellian basin. Around the K/Pg boundary, a new compressional episode affected the northern African-Arabian Fold Belt (Guiraud and Bosworth 1997; Guiraud 1998). The Tellian domain recorded this compressional phase, which is probably preparatory for the emplacement of the local thrusting during the Miocene. This tectonic evolution is related to the convergence of the African and European plates and the closure of the south-western Tethyan. The K/Pg boundary compressional event caused that the Danian deposits are very rare throughout the Tellian basin, which are essentially marls rich in microfauna. Nevertheless, the Maastrichtian and Danian deposits of the Tellian basin are lithologically inseparable. The southern part of the Tellian basin contains epi-neritic facies, which laterally change towards the deepest deposits of the center of the basin. This central part shows the base of infra-neritic facies, which change towards bathyal facies, such as marls with yellow calcareous nodules of the subunit VIc. Detrital inputs are more abundant and coarser the closer to the northern edge of the Tellian basin. The presence of detrital formations in the northern part of the basin indicates embryonic tectonic that affects internal areas around the K/Pg boundary.

Lithostratigraphy

The Souagui region is characterized by thick allochthonous deposits of Cretaceous to Eocene age (Kieken 1974), consisting of marls with intercalation of limestones (Fig. 2). According to Kieken (1974), three main litho-stratigraphic units can be recognized in this region: 1) Unit I: It outcrops along the northern slope of Djebel Chaâba mountain and is characterized of monotonous marly facies; two formations can be recognized: a lower one, ~200 m thick and consisting of clays and laminated marls with black limestone lenses, and a upper one, ~1000 m thick and consisting of dark or blue gray marls with intercalations of yellowish marly limestones; 2) Unit II: It outcrops to the south of Unit I and consists of ~50 m thick blue-black pyritic marls; and 3) Unit III: It outcrops along the highest part of the Djebel Safah region, forming massive limestone cliffs, and consists of an alternation of light gray/white limestones with black silex nodules and light gray marls.

The Sidi Ziane and Djebel Zakhamoune sections belong to the Unit I, which is Maastrichtian to Danian in age (Fig. 3). Both sections exhibit similar lithological characteristics, and two stratigraphic subunits can be recognized:

- Upper Maastrichtian Subunit: It consists of clayey marls, yellowish or bluish light gray in the lower part and dark gray in the upper part. The uppermost 18.5 meters of this subunit were sampled in Sidi Ziane and the uppermost 26 meters in Djebel Zakhamoune. The clayey marls in the lower part of the subunit are sometimes hard, schistose and organized in centimeter levels. Intervals with calcareous marls and/or marly limestones intercalated with clayey marls are also recognized. In Sidi Ziane, a bioturbated level rich in oxidized millimeter-burrows has been found about 10 m below the K/Pg boundary. The dark clayey marls of the upper part of the subunit are hardened and apparently laminated (interval of lithofacies C, Fig. 3), with a content of 30% $CaCO_3$.
- Lower Danian Subunit: It mainly consists of an alternation of dark clayey marls and beige marly limestones. More of 100 m of this subunit were sampled in both Sidi Ziane and Djebel Zakhamoune sections. Its lower part is characterized by black clayey marls with 15 cm-diameter gray nodules of barite. The dark clayey marls have a content of 30% $CaCO_3$. The limestones beds have nodular appearance and dolomitic and microsparitic texture, and contain some ferruginized bioclasts.

Two types of lithofacies have been distinguished in both subunits: lithofacies A, predominantly dark clayey marly, and lithofacies B, with intercalations of marly limestones and marls (Fig. 3). These two types of facies have allowed us to identify lithozones A_M and B_M and A_D and B_D (M= Maastrichtian; D = Danian) in both Sidi Ziane and Djebel Zakhamoune sections, as well as a lithozone C for hardened clayey marls of the upper part of Upper Maastrichtian Subunit (Fig. 3). Because the uppermost Maastrichtian and lowermost Danian have similar lithostratigraphic characteristics in both sections, the identification of the K/Pg boundary in Sidi Ziane and Djebel Zakhamoune is difficult without the help of a detail planktic foraminiferal biostratigraphy. Nevertheless, the presence of distinctive limestone beds in Danian deposits immediately above the K/Pg boundary (2.5 m in Sidi Ziane and 4.5 m in Djebel Zakhamoune) can be used as key lithohorizon (base of lithozone A_{D1}, Fig. 3).

Material and methods

For biostratigraphic studies with planktic foraminifera, 144 samples at Sidi Ziane and 91 samples at Djebel Zakhamoune across the critical K/Pg boundary interval were collected. The uppermost Maastrichtian and the lowermost Danian stratigraphic interval were sampled at high-resolution, i.e., at 2 cm immediately below and above the K/Pg boundary, and decreasing resolution (10, 25, 50, 100, 200 and 500 cm) further away from the boundary. Samples were processed using standard disaggregating technique employing diluted H_2O_2. All samples were dried at ≤50°C, and sieved into 63 μm, 160 μm, 400 μm and 1 mm size fractions. For the biostratigraphic study, the most relevant species of the K-Pg transition were intensively searched in all samples from ≥63 μm size fraction. All samples are rich in planktic foraminifera, whose preservation is good enough to perform precise biostratigraphic studies. Some relevant specimens were examined and photographed under Zeiss MERLIN FE-SEM scanning electron microscope (SEM) at the Universidad de Zaragoza (Spain).

The Algerian sections have been compared with four of the most complete and continuous sections of the K-Pg transition in the western Tethys (Fig. 4): Bottaccione (Gubbio, Italy), Agost and Caravaca (Spain), and Kalaat Senan (Tunisia). Biostratigraphic data of these four sections have been revised again to take into account the novelties related to planktic foraminiferal taxonomy of the lower Danian (see Arenillas et al. 2018) and that affect the stratigraphic ranges assigned to the some index-species in previous studies. The K/Pg boundary is marked in all of them by an Iridium-rich layer (Alvarez et al. 1980; Smit and Hertogen 1980; Smit 1982; Dupuis et al. 2001). The K/Pg boundary was defined in fact at the base of the Iridium-rich layer in the El Kef stratotype, coinciding with the planktic foraminiferal catastrophic mass extinction (Molina et al. 2006). This layer is placed at the base of the informally known as K/Pg Boundary Clay, which is composed of two beds in continuous Tethyan sections: (1) a millimeter-thick ejecta-rich airfall layer, usually reddish, with high concentrations of Iridium, and (2) a dark clay bed with low values in $\delta^{13}C$. Estimated durations for their deposition are 1-3 years and 10 kyr respectively (Mukhopadhyay et al. 2001; Arenillas et al. 2006).

Gubbio depicts one of the classic European localities for the chronostratigraphic study of the upper Cretaceous and lower Paleogene. Near Gubbio, there are two well-known sections (Bottaccione and Contessa -currently Contessa Highway-), which have historically been very important for the correlation between the planktic foraminiferal zonation (Luterbacher 1964, 1975; Luterbacher and Premoli Silva 1964; Premoli Silva et al. 1976; Premoli Silva and Sliter 1995) and the magnetostratigraphic scale (Alvarez et al. 1977; Premoli Silva et al. 1980; Lowrie et al. 1982). The

foraminiferal preservation is very poor, but enough to carry out precise biostratigraphic studies. The K-Pg transition in both Gubbio sections consists mainly of pelagic limestones of the Scaglia Rossa Formation (Umbria-Marche Apennines, central Italy). The K/Pg boundary is marked by a 1 cm-thick airfall layer, green toward the base and red toward the top, which is devoid of planktic foraminifera. It contains microspherules, schocked quartz, and Ni-rich spinels, as well as an anomalous Iridium concentration of up to 8 ppb (Montanari 1991; Smit 1999). The dark clay bed has not been found in the Gubbio sections, suggesting a small hiatus similar to that identified from the nearby Ceselli section (Arenillas and Arz 2000). Nevertheless, the airfall layer in Bottaccione and Contessa could really be a condensed level that includes both airfall layer and dark clay bed. Arenillas (1998) reviewed the Paleocene and lower Eocene planktic foraminiferal biostratigraphy of Bottaccione and Contessa sections using samples previously studied by Luterbacher (1964) and deposited at the Institut und Museum für Geologie und Paläontologie of the Universität Tübingen (Germany). Recently, Gardin et al. (2012), Galeotti et al. (2015) and Coccioni and Premoli Silva (2015) have revised in Gubbio the correlation between the planktic foraminiferal biostratigraphy and the magnetostratigraphy for the Upper Cretaceous and Paleocene.

The Agost section (Betic Cordillera, SE Spain) was used by Arenillas et al. (2004) as the reference section to establish their early Danian biochronological scale with planktic foraminifera. The K-Pg transition in Agost consists mainly of hemipelagic marls and marly limestones of the classical Jorquera (Van Veen 1969) and Quipar-Jorquera Formations (Vera et al. 1982). The upper Maastrichtian interval at Agost was redefined as the Raspay Formation by Chacon (2002) and the Danian-lower Selandian interval as the Agost Formation (Chacón and Martín-Chilevet, 2005). The foraminiferal preservation is moderately good. The K/Pg boundary is marked by a 1 to 2 mm-thick airfall layer, which contains microspherules, schocked quartz, and Ni-rich spinels, as well as an anomalous Iridium concentration of up to 24.4 ppb (Martínez-Ruiz et al. 1992, 1997). The dark clay bed is 10 to 12 cm-thick, but it is especially dark in its first 4 to 5 cm. Arenillas et al. (2004) chose this locality as reference section for their K-Pg transition biochronological scale because detailed studies of the planktic foraminiferal biostratigraphy (Arz 1996; Arenillas 1996; Molina et al. 1996, 1998, 2005) and the magnetostratigraphy (Groot et al. 1989) were previously carried out across the K/Pg boundary.

The Caravaca section (Betic Cordillera, SE Spain) stands for one of the classic localities for the study of the K/Pg boundary (Smit 1982, 2004). The K-Pg transition in Caravaca consists mainly of

hemipelagic marls and marly limestones of the classical Jorquera Formation (Van Veen 1969). As at Agost, the upper Maastrichtian interval was redefined at Caravaca as the Raspay Formation (Chacon 2002) and the Paleocene interval as the Agost Formation (Chacón and Martín-Chilevet 2005). The foraminiferal preservation is moderately good. The K/Pg boundary is marked by a 1 to 2 mm thick airfall layer, which contains microspherules, schocked quartz, and Ni-rich spinels, as well as an anomalous Iridium concentration of up to 56 ppb (Martínez-Ruiz et al. 1997; Kaiho et al. 1999; Smit 2004). The dark clay bed is 8 to 10 cm thick, and it is especially dark in its first 2 to 3 cm. The planktic foraminiferal biostratigraphy of the K-Pg transition was studied by Canudo et al. (1991), Arz (1996), Arenillas (1996), Arenillas and Molina (1997) and Arz et al. (2000). Magnetostratigraphic data in Caravaca were obtained by G. Brunsmann (after Smit 1982) and compared with those of Bottaccione (Alvarez et al. 1977) and Agost (Groot et al. 1989). The Caravaca section was chosen as an auxiliary section of the GSSP for the K/Pg boundary (Molina et al. 2009).

The Kalaat Senan area (central-west Tunisia) is placed 50 Km south of the GSSP of K/Pg boundary at El Kef, Tunisia (Molina et al. 2009). The K-Pg transition in Kalaat Senan consists mainly of hemipelagic marls of the Haria Formation (Aurès Atlas Mountains). It includes two localities: Aïn Settara for the Upper Maastrichtian and lower Danian (Arz 1996; Arenillas 1996; Arenillas et al. 2000b; Dupuis et al. 2001), and Sidi Nasseur for the middle to upper Danian (Arenillas 1996; Steurbaut et al. 2000). The K-Pg transition in Kalaat Senan has a high sedimentation rate, with an average of 6 cm/kyr according to Steurbaut et al. (2000). The foraminiferal preservation is good to very good, and occasionally excellent in Sidi Nasseur. At Aïn Settara, the K/Pg boundary is marked by a 1 to 5 mm-thick airfall layer, consisting of yellowish, jarositic platy nodules. It contains microspherules, schocked quartz, and Ni-rich spinels, as well as an anomalous Iridium concentration of up to 11 ppb (Dupuis et al. 2001). The dark clay bed is 55 cm thick, but it is especially dark in its first 15 cm. A silt bed, with channel-like structures and probable ripples in its top, was identified in 3-5 cm above the K/Pg boundary. It was interpreted as a single storm deposit (Dupuis et al. 2001), but probably not related to the K/Pg boundary event. The Aïn Settara section was chosen as other auxiliary section of the GSSP for the K/Pg boundary (Molina et al. 2009).

For the biochronological calibrations of planktic foraminiferal events (first and last appearances of index-species), we have used the Geological Times Scale GTS2012 of Gradstein et al. (2012). According to this scale, the K/Pg boundary is about 66.040 Ma in age, and the C30n/C29r and C29r/C29n boundaries occurred respectively 358 kyrs before the K/Pg boundary and 352 kyr after the K/Pg

boundary. The rest of boundaries between (magneto-) chrones occurred as indicated in Table 1. Magnetochronological calibrations are constantly being adjusted and, for example, it has recently been estimated that the K/Pg boundary is about 66.052 Ma in age, the C30n/C29r boundary occurred 259 kyrs before the K/Pg boundary, and the C29r/C29n boundary 328 kyr after the K/Pg boundary (Sprain et al. 2018). These adjustments alter the biochronological calibrations proposed here. However, since Sprain et al. (2018) study does not span the entire interval studied in the Médéa area, we have continued using the scale GTS2012 with the purpose of simplifying the chronological information.

Planktic foraminiferal zonation

Upper Maastrichtian planktic foraminiferal zonation

For the uppermost Maastrichtian, we have used the planktic foraminiferal zonation of Li and Keller (1998), of alphanumeric nomenclature, because it is the highest resolution biozonation described so far for tropical-subtropical latitudes (Fig. 5). These authors divided the standard biozones of Caron (1985) for the uppermost Maastrichtian, i.e. *Abathomphalus mayaroensis* Zone and uppermost part of *Gansserina gansseri* Zone, in four biozones (from top to base): Zones CF1 (of *Plummerita hantkeninoides*), CF2 (of *Pseudoguembelina palpebra*), CF3 (of *Pseudoguembelina hariaensis*) and CF4 (of *Racemiguembelina fructicosa*). It has been compared with the zonation of Arz and Molina (2002), which divided this interval in four biozones (from top to base): *Plummerita hantkeninoides*, *Pseudoguembelina hariaensis*, *Abathomphalus mayaroensis,* and *Racemiguembelina fructicosa* Zones. This biozonation was set up after detailed biostratigraphic studies synthesized in the Doctoral Thesis of Arz (1996), and based on the taxonomic schemes of Robaszynski et al. (1983-1984), Caron (1985) and Nederbragt (1990). The Zone CF4 is equivalent to the *R. fructicosa* and *A. mayaroensis* Zones of Arz and Molina (2002), Zones CF2 and CF3 spans the same biostratigraphic interval as the *Psg. hariaensis* Zone, and Zone CF1 is equivalent to the *Pt. hantkeninoides* Zone (Fig. 5). The index-species and some relevant species of the uppermost Maastrichtian are illustrated in the Fig. 6 and described in the Appendix 1.

In the Sidi Ziane and Djebel Zakhamoune sections, only the last two biozones of the Upper Maastrichtian zonation of Li and Keller (1998) and Arz and Molina (2002) have been identified. In addition the mass extinction horizon at the K/Pg boundary, the used key-biohorizons were the Highest

Occurrence Datum (HOD) of *Gs. gansseri* and Lowest Occurrence Datum (LOD) of *Pt. hantkeninoides*, as described below:

Zone CF2 or Pseudoguembelina palpebra Interval Zone (upper part of Pseudoguembelina hariaensis Zone of Arz and Molina 2002)

Definition: The interval between the HOD of *Gansserina gansseri* and the LOD of *Plummerita hantkeninoides*

Author: Li and Keller (1998)

Remarks: Nederbragt (1990) defined the *Pseudoguembelina hariaensis* Zone in order to characterize the uppermost Maastrichtian, i.e. up to the K/Pg boundary. It was used with the same meaning in other relevant biozonations such as those of Robaszynski and Caron (1995) and Huber et al. (2008). Arz and Molina (2002) modified its upper boundary to place it at the LOD of *Pt. hantkeninoides* with the aim of further increasing the resolution of the upper Maastrichtian biostratigraphic scales. However, because the paleobiogeographical distribution of *Pt. hantkeninoides* was restricted to practically tropical-subtropical latitudes, the original definition of *Psg. hariaensis* Zone is usually used for higher latitudes (Huber et al. 2008; Pérez-Rodríguez et al. 2012). Li and Keller (1998) divided the *Pseudoguembelina hariaensis* Zone of Nederbragt (1990) into two: Zones CF2 and CF3, using the LOD of *Gs. gansseri* as boundary between them.

Zone CF1 or Plummerita hantkeninoides Taxon-range Zone

Definition: The interval between the LOD and HOD of *Plummerita hantkeninoides*

Author: Ion and Szasz (1994)

Remarks: Ion and Szasz (1994) defined this biozone in order to characterize the uppermost Maastrichtian in localities from tropical-subtropical latitudes. The utility of *Pt. hantkeninoides* as index-species loses validity for higher latitudes, such as pointed out by Arz and Molina (2002) and Pérez-Rodríguez et al. (2012). Nevertheless, this biozone has a great interest in the Tethys region because it allows characterizing the uppermost Maastrichtian, thus increasing the resolution of the biostratigraphic scales in this critical interval prior to the K/Pg boundary mass extinction.

Lower-Middle Danian planktic foraminiferal zonation

For the Danian, we have used the planktic foraminiferal zonations of Arenillas and Molina (1997) and Arenillas et al. (2004) (Fig. 5), which were based respectively on those of Toumarkine and Luterbacher (1985) and Molina et al. (1996). They have been compared with the most standard zonation of Berggren and Pearson (2005), of alphanumeric notation, which was recently revised by Wade et al. (2011), since these are the most commonly used in the Paleogene biostratigraphy and chronostratigraphy. It should be noted that there is a set of discrepancies between both biostratigraphic scales due to differences in the diagnostic criteria assigned to some index-species. Arenillas and Molina (1997) and Arenillas et al. (2004) scales for the Danian were mainly based on the taxonomic schemes of Bolli (1957, 1966), Luterbacher (1964), Luterbacher and Premoli Silva (1964), Stainforth et al. (1975), Blow (1979) and Toumarkine and Luterbacher (1985), which were synthesized in the Doctoral Thesis of Arenillas (1996) and updated in later works of the author. The index-species and some relevant species of the lower and middle Danian are illustrated in the Fig. 6 and described in the Appendix 1. The Berggren and Pearson (2005) biozonation for the Danian, as previous and subsequent zonations of the authors (Berggren and Miller 1988; Berggren et al. 1995; Wade et al. 2011), is based on the taxonomic schemes of Berggren (1977), Berggren and Norris (1997) and Olsson et al. (1999). The taxonomy of the latter differs in some relevant points with respect to the more traditional taxonomy of Bolli (1957, 1966), Luterbacher (1964), Stainforth et al. (1975) and Toumarkine and Luterbacher (1985), affecting the taxonomic sense of some index-species (mainly the diagnostic characters assigned to the index-species *Parvularugoglobigerina eugubina* and *Acarinina trinidadensis*). In general terms, Arenillas (1996) taxonomy is more splitter than that of Olsson et al. (1999). These discrepancies are described below in order to better understand differences between the biostratigraphic scale used here and the more standardized scale of Berggren and Pearson (2005). Similar biozonations with alphanumeric nomenclature were defined by Blow (1979), Smit (1982), Keller (1988, 1993) and Keller et al. (1995), which have generated confusion with the notation "P" of the biozones defined in the lower Danian (see Fig. 5).

Although only the last biozones have been identified in the Sidi Ziane and Djebel Zakhamoune sections, we describe below the five biozones of Arenillas and Molina (1997) and Arenillas et al. (2004) for the lower-middle Danian. In addition the mass extinction horizon at the K/Pg boundary, the used key-biohorizons were the LODs of *Parvularugoglobigerina longiapertura*, *Parvularugoglobigerina*

eugubina, *Eoglobigerina simplicissima*, *Parasubbotina pseudobulloides*, *Subbotina triloculinoides*, *Globanomalina compressa*, *Acarinina trinidadensis* and *Acarinina uncinata*, as described below:

Guembelitria cretacea Interval Zone

Definition: The interval between the HODs of *Plummerita hantkeninoides* and *Abathomphalus mayaroensis* (= K/Pg boundary) and the LOD of *Parvularugoglobigerina eugubina*

Author: Molina et al. (1996)

Remarks: The *Gb. cretacea* Zone of Arenillas et al. (2004) is not equivalent to the Zone P0 of Smit (1982), which was defined in the type-locality of Caravaca, Spain, as the interval between the K/Pg boundary and the LOD of *Globigerina minutula* (= *Palaeoglobigerina alticonusa* in this paper). This key-biohorizon is correlatable to the LOD of *Parvularugoglobigerina longiapertura* of the Arenillas et al. (2004) biozonation, but not to the LOD of *Parvularugoglobigerina eugubina* as suggested by Smit (1982). The *Gb. cretacea* Zone of Arenillas et al. (2004) is also not correlatable to the Zone P0 of Berggren and Pearson (2005), because they considered, as Smit (1982), that *Pv. longiapertura* is a junior synonym of *Pv. eugubina*. Arenillas et al. (2004) divided the biozone in two subbiozones:

(1) *Muricohedbergella holmdelensis* Interval Subzone (Zone P0 of Smit 1982)

Definition: Interval between the HODs of *Plummerita hantkeninoides* and *Abathomphalus mayaroensis* to the LOD of *Parvularugoglobigerina longiapertura*

Author: Arenillas et al. (2004)

Remarks: This subbiozone is equivalent to the Zone P0 of Smit (1982) except that Arenillas et al. (2004) defined its upper boundary with the LOD of *Pv. longiapertura* instead of the correlatable LOD of *Globigerina*? *minutula* (= *Pg. alticonusa* in this paper). It is characterized exclusively by species surviving the mass extinction event of the K/Pg boundary. Arenillas et al. (2004) used *Mh. holmdelensis* as the nominate species for the subzone, because this species is considered a probable survivor (see Olsson et al. 1999). According to the biostratigraphic scheme of Smit (1982), those studies that include species of the genera *Parvularugoglobigerina*, *Globoconusa*, *Eoglobigerina*, *Parasubbotina*, *Praemurica* and/or *Globanomalina* within the Zone P0 or *Mh. holmdelensis* Subzone are inaccurate (see Arenillas et

al. 2004), and probably based on localities with hiatuses or condensed levels affecting the K/Pg boundary and/or localities affected by problems of reworking, mixture and/or infiltration.

(2) *Parvularugoglobigerina longiapertura* Interval Subzone

Definition: The interval from the LOD of *Parvularugoglobigerina longiapertura* to the LOD of *Parvularugoglobigerina eugubina*

Author: Arenillas et al. (2004)

Remarks: As Blow (1979), Canudo et al. (1991) and Apellaniz et al. (1997), Arenillas et al. (2004) used *Pv. longiapertura* as index-species. This species has a very distinct morphology, with a high slit-like aperture unlike the true *Pv. eugubina* (see Appendix 1). However, Olsson et al. (1999) considered it a junior synonym of the latter (see Fig. 5). This fact may have probably caused a long confusion among the Danian planktic foraminiferal specialists in the use of the Zone P0 of Berggren and Pearson (2005). Keller (1988, 1993) and Keller et al. (1995) distinguished both species, but considered the LODs of *Pv. longiapertura* and *Pv. eugubina* are synchronous (see Fig. 5).

Parvularugoglobigerina eugubina Interval Zone (~ Zone Pα of Berggren and Pearson 2005)

Definition: The interval from the LOD of *Parvularugoglobigerina eugubina* to the LOD of *Parasubbotina pseudobulloides*

Author: Luterbacher and Premoli Silva (1964), emended by Bolli (1966)

Remarks: The *Pv. eugubina* Zone of Arenillas et al. (2004) is not strictly equivalent to the *Globigerina eugubina* Zone of Luterbacher and Premoli Silva (1964), which was originally defined in the type-locality of Gubbio, Italy, as the interval of total range of *Globigerina eugubina* (= *Parvularugoglobigerina eugubina* in this paper). This definition was maintained by Toumarkine and Luterbacher (1985), and also by Berggren and Miller (1988), Berggren et al. (1995), Berggren and Pearson (2005) and Wade et al. (2011) for their equivalent Zone Pα. Bolli (1966) emended its upper boundary placing it in the LOD of *P. pseudobulloides*, such as Canudo and Molina (1992), Molina et al. (1996) and Arenillas et al. (2004) did later. Since the zonation of Berggren and Pearson (2005) was based on the taxonomy of Olsson et al. (1999), they considered that *Pv. eugubina* spans the diagnostic characters of *Pv. longiapertura*, *Pv. sabina, Trochoguembelitria liuae* and *T. olssoni*, in addition to those of the real *Pv. eugubina* (see

Arenillas et al. 2016; Arenillas and Arz 2017). The first two species are older and, like *Pv. eugubina*, have a microperforate smooth wall; the last two are younger and have a rugose and/or pore-mounded wall. The Zone Pα of Berggren and Pearson (2005) is therefore conceptually equivalent to the *Pv. eugubina* Zone of Toumarkine and Luterbacher (1985) and Arenillas et al. (2004) but spans a different biochronostratigraphic interval (see Fig. 5). The Zone Pα of Berggren and Pearson (2005) probably spans not only the *Pv. longiapertura* Subzone and *Pv. eugubina* Zone, but also the *E. trivialis* Subzone of Arenillas et al. (2004), because the LOD of *T. liuae* is approximately placed at the top of this last subbiozone (see Fig. 5). The Zone Pα of Blow (1979) and the *Pv. longiapertura* Zone of Canudo et al. (1991) are also equivalent to the *Pv. eugubina* Zone, but their bases were placed at the LOD of *Pv. longiapertura*, spanning therefore both *Pv. longiapertura* Subzone and *Pv. eugubina* Zone of Arenillas et al. (2004). Similarly, the Subzone P1a of Keller (1988, 1993) and Keller et al. (1995) is equivalent to the *Pv. eugubina* Zone, although they considered that the LODs of *Pv. longiapertura* and *Pv. eugubina* are coincident, thereby also spanning the *Pv. longiapertura* Subzone.

The latter divided the *Pv. eugubina* Zone in two subbiozones:

(1) *Parvularugoglobigerina sabina* Interval Subzone (~ Subzone P1a of Smit 1982)

Definition: The interval ranging from the LOD of *Parvularugoglobigerina eugubina* to the LOD of *Eoglobigerina simplicissima*.

Author: Arenillas et al. (2004)

Remarks: Stainforth et al. (1975), Toumarkine and Luterbacher (1985) and Olsson et al. (1999) considered *Pv. sabina* as a junior synonym of *Pv. eugubina*. However, Arenillas and Arz (2000) distinguished them according to the original meaning given to both species by Luterbacher and Premoli Silva (1964), such as described in the Appendix 1. This proposal was made after a new inspection of the holotypes of both species deposited in the collections of the Naturhistorisches Museum of Basel (Switzerland), as well as the type-sample where were defined both holotypes from Ceselli (Italy) and the type-sample of *Pv. eugubina* Zone from Gubbio (Italy). Both type-samples were deposited in the HansPeter Luterbacher collections of the Institut und Museum für Geologie und Paläontologie. Universität Tübingen (Germany) (see Arenillas and Arz 2000).

(2) *Eoglobigerina simplicissima* Interval Subzone (~ lower part of the Subzone P1b of Smit 1982)

Definition: The interval between the LOD of *Eoglobigerina simplicissima* and the LOD of *Parasubbotina pseudobulloides*.

Author: Arenillas et al. (2004)

Remarks: Arenillas et al. (2004) established this subzone to include in the planktic foraminiferal zonations a very relevant key-biohorizon: the first record of Danian species with pitted/cancellate wall texture (see Arenillas and Arz 2013a,b). The planktic foraminifers reach "normal" size in this subzone and thus can be found in the fraction larger than 150 microns. This key-biohorizon was already utilized similarly by Smit (1982) to define his Subzone P1b (see Fig. 5), although using instead the LOD of *Eoglobigerina taurica* (= *Praemurica taurica* in this paper) as key-biohorizon. Arenillas et al. (2004) used to *E. simplicissima* as index-species, since it is the first Danian species in appear with a pitted/cancellate wall texture. Olsson et al. (1999) considered *E. simplicissima* as a junior synonym of *Eoglobigerina eobulloides*, but Arenillas et al. (2004) used it for the name of the subzone because this species has a more distinctive and stable morphology than *E. eobulloides* (see Fig. 6, and Appendix 1).

Parasubbotina pseudobulloides Interval Zone (~ Zone P1 of Berggren and Pearson 2005)

Definition: The interval between the LOD of *Parasubbotina pseudobulloides* and LOD of *Globanomalina compressa*.

Author: Leonov & Alimarina (1961), called *Globigerina pseudobulloides-Globigerina daubjergensis* Zone; emended by Molina et al. (1996)

Remarks: *Parasubbotina pseudobulloides* is an index-species used in most planktic foraminiferal zonations of the Danian (Bolli 1966; Smit 1982; Toumarkine and Luterbacher 1985; Canudo and Molina 1992; Arenillas et al. 2004; Berggren and Pearson 2005). There is some uncertainty to place the LOD of *P. pseudobulloides* due to the typical cancellate wall of *Parasubbotina*, as well as *Eoglobigerina*, appeared approximately coinciding with the base of this biozone, exhibiting the first representatives of both genera in the *E. simplicissima* Subzone a rather more smoothed pitted wall, and probably not spinose (Arenillas and Arz 2013b). Olsson et al. (1999) used the name *Parasubbotina* aff. *pseudobulloides* to refer to those specimens similar to *P. pseudobulloides* but with pitted wall. Blow (1979) includes them in *Globorotalia* (*Turborotalia*) cf. *subquadrata* and Arenillas (1996) in *Parasubbotina moskvini*. The *P.*

pseudobulloides Zone is equivalent to the *Globigerina* (*Turborotalia*) *pseudobulloides*/*Eoglobigerina eobulloides simplicissima* (P1) Zone of Blow (1979), who divided it into two subbiozones using the LOD of *G. compressa* as boundary between them: *G.* (*T.*) *pseudobulloides*/*G.* (*T.*) *archaeocompressa* (P1a) and *G.* (*T.) compressa*/*Eoglobigerina eobulloides simplicissima* (P1b) Subzones. Using the same key-biohorizon, Molina et al. (1996) divided it into two biozones, namely *P. pseudobulloides* and *G. compressa* Zones. Later, Arenillas and Molina (1997) and Arenillas et al. (2004) divided it in three subbiozones:

(1) *Eoglobigerina trivialis* Interval Subzone (~ Subzone P1a of Berggren and Pearson 2005)

Definition: The interval from the LOD of *Parasubbotina pseudobulloides* to the LOD of *Subbotina triloculinoides*.

Author: Arenillas et al. (2004)

Remarks: The index-species chosen by Arenillas et al. (2004) to nominate this subzone, *Eoglobigerina trivialis*, was applied by Olsson et al. (1999) in a different taxonomic sense (as belonging to the genus *Subbotina*). Arenillas (2011, 2012) noticed this fact, renaming the species as *Eoglobigerina* cf. *trivialis* (pending definition) in order to refer to the morphotypes illustrated by Blow (1979), which are similar to some of the paratypes of *trivialis*. The Subzone P1b of Keller (1988, 1993) and Keller et al. (1995) may be equivalent to the *E. trivialis* Subzone.

(2) *Subbotina triloculinoides* Interval Subzone (~ Subzone P1b of Berggren and Pearson 2005)

Definition: The interval from the LOD of *Subbotina triloculinoides* to the LOD of *Globanomalina compressa*.

Author: Berggren (1969), emended by Arenillas et al. (2004)

Remarks: Berggren (1969), Berggren and Miller (1988) and Berggren and Pearson (2005) used the LOD of *Subbotina triloculinoides* as the key-biohorizon for the base of their Subzone P1b. However, this subzone is not identical to it used by Arenillas et al. (2004), since Berggren and Pearson (2005) considered the LOD of *G. compressa* (top of P1b) to be within the chron C28n coinciding with the LOD of *Praemurica inconstans* (see discussion below), a datum that probably is equivalent to the LOD of *Acarinina trinidadensis* of Toumarkine and Luterbacher (1985). Therefore the *Subbotina triloculinoides* Subzone probably corresponds biostratigraphically with the lower part of Subzone P1b of Berggren and

Pearson (2005). In addition, Berggren and Pearson (2005) placed the LOD of *Subbotina triloculinoides* in the middle part of C29n. However, bio-magnetostratigraphic correlations by Arenillas et al. (2004) strongly suggest that it is placed in the uppermost part of C29r. The Subzone P1b of Berggren and Pearson (2005) should not be confused with those of Smit (1982) and Keller (1988, 1993), which comprise different biostratigraphic intervals (see Fig. 5).

(3) *Globanomalina compressa* Interval Subzone (~ lower part of the Subzone P1c of Berggren and Pearson 2005)

Definition: The interval from the LOD of *Globanomalina compressa* to the LOD of *Acarinina trinidadensis*.

Author: Blow (1969) and Berggren (1969), emended by Arenillas and Molina (1997)

Remarks: Arenillas and Molina (1997) considered this subbiozone with the rank of biozone. It is equivalent to the Subzone P1c of Berggren and Miller (1988), Berggren et al. (1995) and Berggren and Pearson (2005), the *G. (T.) compressa/Eoglobigerina eobulloides simplicissima* (P1b) Subzone of Blow (1979), and the *G. compressa* Zone of Molina et al. (1996). *G. compressa* have some taxonomic problems because it belongs to an evolutionary lineage whose interspecific boundaries present a certain degree of uncertainty and subjectivity. According to criteria used for *Globanomalina* by Arenillas (1996), mainly based on Blow (1979) and Canudo (1994), this lineage includes the following species from oldest to youngest: *Globanomalina archaecompressa* → *G. planocompressa* → *G. compressa* → *G. haunsbergensis* → *Luterbacheria ehrenbergi* (Arenillas 1996). Olsson et al. (1999) used very similar interspecific boundaries, but they did not consider the keeled genus *Luterbacheria*, and considered *haunsbergensis* a junior synonym of *ehrenbergi*, probably including the *haunsbergensis*-type shapes (with not keeled, moderately to strongly angular periphery) within the interspecific variability of *G. compressa*. The lower part of the Subzone P1c of Keller (1988, 1993) and Keller et al. (1995) may be equivalent to the *G. compressa* Subzone. These taxonomic discrepancies seem to be reflected in the different stratigraphic ranges proposed by Arenillas et al. (2004) and Berggren and Pearson (2005), since the first ones placed the LOD of *G. compressa* in chron C29n, and the last ones placed it in chron C28n. The upper part of the Subzones P1c of Smit (1982), Keller (1988, 1993) and Keller et al. (1995) may be equivalent to the *G. compressa* Subzone.

Acarinina trinidadensis Interval Zone (~ upper part of the Subzone P1c of Berggren and Pearson 2005)

Definition: The interval from the LOD of *Acarinina trinidadensis* to the LOD of *Acarinina uncinata*.

Author: Bolli (1957)

Remarks: As in the previous case, *Ac. trinidadensis* also has taxonomic problems because it belongs to an evolutionary lineage (*Praemurica taurica* → *Pr. pseudoinconstans* → *Pr. inconstans* → *Ac. trinidadensis* → *Ac. uncinata*) whose interspecific boundaries present a high degree of uncertainty and subjectivity (Arenillas 1996; Arenillas and Arz 2013a). This lineage tends to the acquisition of more conical chambers and a muricate wall texture, but its evolution was very gradual preventing clearly establishing the interspecific boundaries in time. According to Bolli (1957), Stainforth et al. (1975), Toumarkine and Luterbacher (1985), Canudo and Molina (1992), Arenillas (1996) and Arenillas and Molina (1997), *Ac. trinidadensis* is an intermediate taxon between *Pr. inconstans* and *Ac. uncinata*, so its lowest occurrence is necessarily younger than the LOD of *Pr. inconstans*. In addition, Arenillas (1996) claimed that *trinidadensis* is the first representative of *Acarinina*, for having a partially muricate wall (observable only when specimens are well-preserved). Conversely, Olsson et al. (1999) suggested that *trinidadensis* is a junior synonym of *inconstans*. This discrepancy causes controversy between the biozonations of Toumarkine and Luterbacher (1985) and Berggren and Pearson (2005). Olsson et al. (1999) assigned probably to *pseudoinconstans* the diagnostic characters assigned to *inconstans* by Toumarkine and Luterbacher (1985). However, the holotype of *pseudoinconstans* chosen by Blow (1979) is indistinguishable from that of *taurica* and probably has some kind of abnormality (underdevelopment of the last three chambers); for this reason, Arenillas (1996), based on Olsson et al. (1992), chose to assign to *pseudoinconstans* the traits of their paratypes as expressed in the Appendix 1, suggesting that it is an intermediate taxon between *Pr. taurica* and *Pr. inconstans* (see Arenillas and Arz 2013a). The Subzones P1d of Smit (1982), Keller (1988, 1993) and Keller et al. (1995) may be equivalent to the *Ac. trinidadensis* Zone.

Acarinina uncinata Interval Zone (~ Zone P2 of Berggren and Pearson 2005)

Definition: The interval between the LOD of *Acarinina uncinata* and LOD of *Morozovella angulata*.

Author: Bolli (1957), emended by Bolli (1966)

Remarks: *Acarinina uncinata* is an index-species used in most biostratigraphic scales (Bolli 1966; Toumarkine and Luterbacher 1985; Berggren and Miller 1988; Canudo and Molina 1992; Berggren et al. 1995; Arenillas and Molina 1997; Berggren and Pearson 2005). It is equivalent to the *Globorotalia* (*Acarinina*) *praecursoria praecursoria* Zone of Blow (1979), who considered *uncinata* a junior synonym of *praecursoria* (both species were defined almost at the same time by Bolli 1957, and Morozova 1957, respectively). Conversely, Olsson et al. (1999) considered *praecursoria* a junior synonym of *uncinata*. However, Luterbacher (1964), Stainforth et al. (1975), Toumarkine and Luterbacher (1985) and Arenillas (1996) distinguished both species by the larger number of chambers of the last whorl in *praecursoria*. Although they noticed that both species represent the same evolutionary lineage and their interspecific boundaries are probably imprecise, the distinction of both species solve this taxonomic and biostratigraphic problem (Arenillas 2011, 2012).

Planktic foraminiferal biostratigraphy in Médéa

Sixty-six species have been identified in the Maastrichtian of Sidi Ziane and Djebel Zakhamoune sections. The Fig. 7 shows the stratigraphic ranges of index-species and some other relevant species in both sections. Some specimens of these species are illustrated in the Figs. 8 and 9. These species belong to the following 19 genera (in alphabetical order): *Abathomphalus, Archaeoglobigerina, Contusotruncana, Globigerinelloides, Globotruncana, Globotruncanella, Globotruncanita, Gublerina, Guembelitria, Heterohelix, Laeviheterohelix, Muricohedbergella, Planoglobulina, Plummerita, Pseudoguembelina, Pseutotextularia, Racemiguembelina, Rugoglobigerina* and *Schackoina*. They depict polytaxic assemblages typical of tropical-subtropical latitudes of the western Tethys during the late Maastrichtian (Arz 1996; Molina et al. 1996, 1998; Arenillas et al. 2000 a, b).

In Sidi Ziane, the LOD of *Pt. hantkeninoides* was identified 1350 cm below the K/Pg boundary. In Djebel Zakhamoune, it was recognized 900 cm below the K/Pg boundary. Therefore, the highest two Maastrichtian biozones (Zones CF2 and CF1) are present in the Médéa area and, in addition, the Zone CF1 has a great thickness if it is compared with other continuous sections of the western Tethys: for example, 140 cm in Botaccione, 345 cm in Agost, or 650 cm in Caravaca. The thickness of the *Pt. hantkeninoides* Zone in Sidi Ziane is equivalent to the most expanded sections of Tunisia: for example 1950 cm in Aïn Settara. These data suggest that both Médéa sections are complete and continuous in the

uppermost Maastrichtian, at least Sidi Ziane. The LOD of *Psg. hariaensis* and HOD of *G. gansseri* are below the stratigraphic interval studied in both Médéa sections. As noteworthy, the HOD of *A. cretacea* was identified 120 cm and 100 cm below the K/Pg boundary of Sidi Ziane and Djebel Zakhamoune respectively. The HOD of *Gs. gansseri* is placed below the studied interval in both sections.

Twenty-nine species have been identified in the Danian of Sidi Ziane and Djebel Zakhamoune. These species belong to the following 10 genera (in alphabetical order): *Acarinina*, *Chiloguembelina*, *Chiloguembelitria*, *Eoglobigerina*, *Globanomalina*, *Globoconusa*, *Parasubbotina*, *Praemurica*, *Subbotina* and *Woodringina*. They depict oligotaxic assemblages typical of lower and middle Danian (Arenillas 1996, 2011, 2012; Arenillas and Molina, 1997; Arenillas et al. 2000 a, b). The stratigraphic ranges and some specimens of the index-species and other relevant species in both sections are showed in Figs. 7, 8 and 9.

At Sidi Ziane, the LODs of *S. triloculinoides* and *G. compressa* were identified coinciding with the K/Pg boundary, indicating a hiatus affecting the lower Danian, specifically the *Gb. cretacea* and *Pv. eugubina* Zones (Zones P0 and Pα), as well as the lower part of the *P. pseudobulloides* Zone (Subzones P1a and P1b). In Djebel Zakhamoune, the hiatus seems to affect a shorter stratigraphic interval because the LOD of *G. compressa* was identified 100 cm above the K/Pg boundary, so that the *S. triloculinoides* Subzone (P1b) is recorded in this section. As noteworthy, the LODs of *Ac. trinidadensis*, *G. haunsbergensis* and *A. uncinata* were respectively identified at about 35, 47 and 68 m above the K/Pg boundary in Sidi Ziane and 48, 66 and 92.5 m above the K/Pg boundary in Djebel Zakhamoune. The LOD of *L. ehrenbergi* was identified 94 m above the K/Pg boundary in Sidi Ziane.

Graphic correlation for planktic foraminiferal biochronology

For the graphic correlation and the dating/calibration of most relevant planktic foraminiferal bioevents of the K-Pg transition, we have revised and correlated four previously studied localities (Agost, Caravaca, Bottaccione and Kalaat Senan) as mentioned above (Fig. 10). A graphic correlation comparing the bio- and magnetohorizons of the Agost, Caravaca, and Bottaccione sections has enabled to accurately calibrate the age of some planktic foraminiferal key-horizons from the uppermost Maastrichtian to the middle Danian, as well as estimate the durations of planktic foraminiferal zones and subzones. This calibration technique will also allow us to obtain a useful biochronological control to evaluate the potential for the

study of the K/Pg boundary mass extinction event and other close paleoenvironmental and paleoclimatic events not only of the Médéa area but also of Algeria. A detailed biochronology of the First and Last Appearances (FA and LA) of the most relevant planktic foraminiferal species for the K-Pg transition is reported in the Table 1.

Lines of correlation (LOCs) were drawn by joining paleomagnetic correlation points of Bottaccione, Agost and Caravaca sections and the geomagnetic polarity time scale (see GTS2012 in Gradstein et al. 2012; Table 1). The K/Pg boundary and magnetic reversals were used as reference points assuming their isochrony. This approach allows us to evaluate the degree of synchrony of planktic foraminiferal horizons across the K/Pg boundary and calibrate the age of the corresponding planktic foraminiferal bioevents.

Biomagnetostratigraphic correlation for the uppermost Maastrichtian and middle Danian

For the calibration in time of key-biohorizons of upper Maastrichtian and middle-upper Danian (Fig. 11A), we chose the Bottaccione section as the Standard Reference Section (SRS), since it is a classic European locality for the chronostratigraphic study of the K-Pg transition (Coccioni and Premoli Silva 2015). Some biostratigraphic data of the Bottaccione section were checked and modified, also taking into account those from the nearby Contessa section (Arenillas 1998). The graphic correlation was revised and corroborated with data from the Caravaca (Fig. 11B, Table 1) and Agost sections (Table 1).

In the uppermost Maastrichtian, The HOD of *Gs. gansseri* and LOD of *Pt. hantkeninoides* were calibrated on average in respectively 428.0 (data from Bottaccione and Agost) and 139.6 kyrs before the K/Pg boundary (data from Bottaccione, Caravaca and Agost). For the graphic correlations of the uppermost Maastrichtian, we also calibrated the HOD of *A. cretacea*, which on average is 12.6 kyrs before the K/Pg boundary (data from Caravaca and Agost). The HOD of *A. cretacea* can be an imprecise datum because the species is very scarce in the late Maastrichtian and could be affected by the Signor-Lipps effect. However, it is the only species considered extinct before the K/Pg boundary during the time interval corresponding to the Zone CF1 (Arz, 1996; Molina et al. 1996; Molina et al. 1998; Gallala 2013).

In the middle-upper Danian, the LODs of *G. compressa, Ac. trinidadensis* and *Ac. uncinata* have been calibrated on average in 640.3, 2043.4 and 3138.4 kyrs after the K/Pg boundary respectively (data from Bottaccione, Caravaca and Agost). For the graphic correlations of the middle-upper Danian, we

have also calibrated the HODs of *G. haunsbergensis* and *L. ehrenbergi*, which on average are 2491.4 and 3937.9 kyrs after the K/Pg boundary respectively (data from Bottaccione, Caravaca and Agost). The HODs of *G. haunsbergensis* and *L. ehrenbergi*, like the HODs of *G. compressa, Ac. trinididadensis* and *Ac. uncinata*, may be problematic data due to the taxonomic uncertainties mentioned above. Nevertheless, they are the most useful data in the biochronological scale with planktic foraminifera of the middle-late Danian.

Biomagnetostratigraphic correlation for the lower Danian

For the calibration in time of lower Danian key-biorizons, we chose the Agost section as the SRS, as did Arenillas et al. (2004) to establish their biochronological scale with planktic foraminifera (Fig. 12A). The graphic correlation was reviewed and corroborated with data from the Caravaca section (Fig. 12B). No biostratigraphic data from the lowermost Danian of Bottaccione has been used because they are still very imprecise. According to this calibration, durations of CF2, CF1*, Gb. cretacea, Pv. eugubina* and *P. pseudobulloides* Zones are respectively 288.4, 139.6, 21.0, 52.8 and 1969.6 kyrs. In the *Gb. cretacea* Zone, average durations of *Mh. holmdelensis* and *Pv. longiapertura* Subzones are respectively 5.6 and 15.4 kyrs. In the *Pv. eugubina* Zone, average durations of *Pv. sabina* and *E. simplicissima* Subzones are respectively 21.9 and 30.9 kyrs. Finally, in the *P. pseudobulloides* Zone, average durations of *E. trivialis* and *S. triloculinoides* Subzones are respectively 174.3 and 392.2 kyrs.

The LODs of *Pv. longiapertura, Pv. eugubina. E. simplicissima, P. pseudobulloides* and *S. triloculinoides* have been calibrated on average in 5.6, 21.0, 42.9, 73.8 and 248.1 kyrs after the K/Pg boundary respectively (data from Agost and Caravaca). As in the previous case, these key-biohorizons may also be problematic due to the taxonomic problems mentioned above. However, this succession of planktic foraminiferal events has been corroborated in the most expanded and continuous sections worldwide, such as El Kef, Aïn Settara and Elles sections (Arenillas 1996; Arz et al. 1999; Arenillas et al. 2000a,b; Molina et al. 2006, 2009).

Graphic correlation for Kalaat Senan (Aïn Settara and Sidi Nasseur)

Given the absence of paleomagnetic data in the Kalaat Senan area (Tunisia), we have used planktic foraminiferal key-horizons, previously calibrated, for the graphic correlation (Fig. 13, Table 2). The graphic correlation suggests high sedimentation rates in both Maastrichtian and Danian intervals. The HOD of *Gs. gansseri* and LOD of *Pt. hantkeninoides* are placed respectively 4600 and 1950 cm below the K/Pg boundary taking into account data from Arz (1996) and Arenillas et al. (2000b). These data imply sedimentation rates of 9.19 and 14.25 cm/kyr for the Zones CF2 and CF1 respectively, with an average of 10.75 cm/kyr for the uppermost Maastrichtian. The HOD of *A. cretacea* is 140 cm below the K/Pg boundary, corroborating that this species could be extinguished before the mass extinction event.

For the Danian, the average sedimentation rate is 5.58 cm/kyr taking into account biostratigraphic data of Arenillas (1996) and Arenillas et al. (2000b). However, there are differences in sedimentation rates depending on the biozones (Table 2). The sedimentation rate is especially high in the *E. simplicissima* Subzone, with 11 cm/kyr. Sedimentation rates are also high in the *Pv. sabina* Subzone and *G. compressa* and *Ac. trinidadensis* Zones, with 6.85, 5.34 and 7.12 cm/kyr respectively. However, they are comparatively low in two stratigraphic intervals: 1) *Mh. holmdelensis* and *Pv. longiapertura* Subzones, with 2.68 and 2.92 cm/kyr respectively, and 2) *E. trivialis* and *S. triloculinoides* Subzones, with 2.87 and 2.93 cm/kyr respectively. Although they are still 3 or 4 times higher than in Caravaca and Agost (see Table 1), the decrease in the sedimentation rate in these two intervals requires an explanation: (1) The thickness of the *Mh. holmdelensis* and *Pv. longiapertura* Subzones in Aïn Settara (15 and 45 cm respectively) are much lower compared to those in the nearby El Kef stratotype: 50 and 150 cm respectively. These thicknesses have a clear correspondence with the thicknesses of the K/Pg boundary dark clay bed in both sections: 55 cm thick in Aïn Settara and about 200 cm in El Kef. In the latter, the dark clay bed consists of 100 cm-thick blackish or dark clay and 100 cm-thick darkened grey marly clay (Molina et al. 2006), and it is characterized by low values in $\delta^{13}C$ and $CaCO_3$ content and high values in total organic carbon or TOC (Keller and Lindinger 1989). Except for the storm deposit identified in 3-5 cm above the K/Pg boundary (Dupuis et al. 2001), there is no biostratigraphic evidence of hiatuses in the dark clay bed of Aïn Settara. Therefore, their lower sedimentation rate is due to a stratigraphic condensation greater than in El Kef, perhaps caused locally by a decrease in the supply of sediments under the post-K/Pg conditions of global climatic warming and alterations in oceanic productivity (see, for example, Birch et al. 2016).

(2) The comparatively lower sedimentation rate in the *E. trivialis* and *S. triloculinoides* Subzones of Aïn Settara suggests not only a greater stratigraphic condensation but also the possible presence of hiatuses undetected in biostratigraphic studies with planktic foraminifera. In the nearby Elles section, a relevant hiatus was identified in the transition between the *Pv. eugubina* and *P. pseudobulloides* Zones (Arz et al. 1999), affecting mainly the *E. simplicissima* and *E. trivialis* Subzones, and the lower part of *S. triloculinoides* Subzone. In the Tunisian sections, this stratigraphic interval affected by hiatuses or lower sediment supply could be related to the warming episode called Dan-C2, which is the first hyperthermal episode of the Paleogene (Quillévéré et al. 2008; Coccioni et al. 2010). The global warming episode Dan-C2 could globally modify the ocean circulation, marine currents, sediment transport and erosion, and locally enhance the development of hiatus and intervals of reduced sedimentation. It is remarkable that, on the contrary, the sedimentation rate in Caravaca increases in the *E. trivialis* and *S. triloculinoides* Subzones with respect to the SRS in Agost (Fig. 12).

Age-depth models for the Médéa sections

Age-depth plots for the Sidi Ziane and Djebel Zakhamoune sections have been set up with LOCs through recognized planktic foraminiferal key-biohorizons. The age model has enabled to estimate the variations of sedimentation rates during the Maastrichtian and Danian and the duration of the hiatus that affects the lower Danian in both sections. In the graphic correlations (Figs. 14 and 15, Table 3), the lower Danian hiatus is represented by a horizontal terrace. Reliable planktic foraminiferal data to establish the LOCs and calculate sedimentation rates are scarce due to the intervals recorded in the Médéa sections (uppermost Maastrichtian and middle Danian) are characterized by great evolutionary stability in the planktic foraminiferal group (Arz 1996; Arenillas 1996, 2011, 2012; Arenillas and Molina 1997; Arz et al. 2000). The LOD of *Pt. hantkeninoides* and the HOD of *A. cretacea*, calibrated respectively in 139.6 and 12.6 kyr before the K/Pg boundary, are the only data available to establish the LOCs in the uppermost Maastrichtian. For the Danian, LODs of *G. compressa*, *Ac. trinididadensis* and *Ac. uncinata* have been used as the key-biohorizons, calibrated respectively in 640.3, 2043.4 and 3138.4 kyrs after the K/Pg boundary.

The LOCs that link the LOD of *Pt. hantkeninoides* and the HOD of *A. cretacea* strongly suggest that the Maastrichtian part is complete and continuous in both Médéa sections. The average sedimentation

rates in the Maastrichtian are 8.98 cm/kyr for Sidi Ziane and 6.58 cm/kyr for Djebel Zakhamoune. Their sedimentation rates are very high compared with those of Bottaccione (1.19 cm/kyr), Agost (2.09 cm/kyr), and Caravaca (4.61 cm/kyr), and equivalent to that of Aïn Settara (10.75 cm/kyr, or 14.25 cm/kyr for the Zone CF1). The hiatus that marks the base of the lower Danian in both sections separates the rest of the Maastrichtian and Danian sequences of apparently continuous deposition.

In Djebel Zakhamoune, the sedimentation rates are 3.35 cm/kyr for the *G. compressa* Subzone and 4.06 cm/kyr for the *Ac. trinidadensis* Zone (Fig. 14, Table 3), with an average of 3.66 cm/kyr for the recorded Danian interval. According to the latter, the lower Danian hiatus has an estimated duration of 732.9 kyr. However, if only the sedimentation rate of the *G. compressa* Subzone is considered for the lowest part of the Danian, the lower Danian hiatus is 610.4 kyr long in Djebel Zakhamoune. This last sedimentation rate is corroborated by the stratigraphic position of the LOD of *G. haunsbergensis* in Djebel Zakhamoune, which adjusts well to the LOC in the *Ac. trinidadensis* Zone.

Because the lower Danian hiatus is more extensive in Sidi Ziane and affect the basal part of the *G. compressa* Subzone, only the sedimentation rate of the *Ac. trinidadensis* Zone (3.01 cm/kyr) is available to estimate that of the studied Danian interval. This rate is corroborated by the stratigraphic position of the LODs of *G. haunsbergensis* and *L. ehrenbergi* in Sidi Ziane, which adjusts well to the LOC in the *Ac. trinidadensis* and *Ac. uncinata* Zones. If this rate is extrapolated to the base of the Danian, the lower Danian hiatus at Sidi Ziane has an estimated duration of 882.0 kyr. However, taking into account the first marly limestone bed of the Danian (base of interval A_{D1}, Fig. 3) as common lithostratigraphic reference point between both sections, the duration of the hiatus in Sidi Ziane seems to be shorter. The base of interval A_{D1} occurs approximately 4.5 m above the K/Pg boundary in Djebel Zakhamoune, but only 2.5 m above the K/Pg boundary in Sidi Ziane. In Djebel Zakhamoune, the base of interval A_{D1} can be calibrated in 744.8 kyr. If this age data is projected graphically to the Sidi Ziane section (Fig. 15), then the average sedimentation rate is lower (2.50 cm/kyr) and the duration of the lower Danian hiatus in this section is shorter (644.9 kyr). Assuming these more realistic calculations for Sidi Ziane, the lower Danian hiatus spans just a little more than the FA of *G. compressa* (640.3 kyr).

The lower Danian hiatus at the studied Médéa sections can have two origins: environmental or tectonic. According to the environmental hypothesis, the hiatus could be related to changes in the sedimentation/erosion rates during the warming episodes post-K/Pg and Dan-C2 (Quillévéré et al. 2008; Coccioni et al. 2010; Arenillas and Arz 2017; Arenillas et al. 2018). According to the tectonic hipothesis,

the hiatus could be related to a small tectonic lifting during the K/Pg boundary compressional event that affects the Tellian basin (Guiraud and Bosworth 1997; Guiraud 1998; Guiraud et al. 2005). In Egypt and Jordan, similar lower Danian hiatuses or unconformities were also recognized (Farouk 2014, 2016) and linked to the K/Pg boundary compressional event as a result of convergence of the African/Arabian Plates toward the Eurasian Plate (Farouk et al. 2014; Farouk and Jain, 2018). Both hypotheses could explain because the uppermost Maastrichtian seems to be complete in the Médéa sections, and why the clayer marls of the uppermost part of Maastrichtian subunit are hardened (lithozone C in Fig. 3). Except for the latter, the Upper Maastrichtian and Danian subunits in Médéa are lithologically indistinguishable. In addition, there are no sedimentary traces of erosion, so the lower Danian hiatus probably depicts an omission surface and non-depositional unconformity (paraconformity). The uppermost Maastrichtian hardened marls can be result of a compaction process (firmground) during the earliest Danian break in sedimentation in the studied Médéa area. This firmground omission surface can therefore be the only lithological criterion of the presence of a hiatus, which stands for a long time gap before the next phase of deposition commenced in the middle Danian.

The identification in the Médéa area of a section more continuous and complete in the lower Danian may be key to interpreting the lower Danian hiatus at Sidi Ziane and Djebel Zakhamoune. The presence of reworked specimens of earliest Danian species *Pv. longiapertura* in both sections (Fig. 7) strongly suggests that the lowermost Danian is recorded in the Médéa area. Nevertheless, the sections studied here, especially Sidi Ziane, may become important for the study of the warming episode LMWE and the planktic foraminiferal extinction pattern before the K/Pg boundary. According the estimated sedimentation rate during the latest Maastrichtian, the 18 meters sampled in Sidi Ziane represent the last 200 kyr of the Maastrichtian (Fig. 15), and sampling can be continued at earlier levels. Bearing in mind that the LMWE occurred between approximately 300 and 150 kyr before the K/Pg boundary according to Barnet et al. (2017), the uppermost part of the LMWE interval (last 50 kyr) have already been sampled.

Conclusions

Two Cretaceous-Paleogene (K-Pg) sections rich in foraminifera (Sidi Ziane and Djebel Zakhamoune) have been found, sampled and studied, standing for the first two K-Pg sections analysed in such detail for of the External Tell System of the Médéa Province, northern Algeria. A detailed study of the planktic

foraminiferal biostratigraphy has revealed the presence of the two last biozones of the Maastrichtian: Zones CF2 and CF1. The thickness of the Zone CF1 (13.5 m in Sidi Ziane and 9 m in Djebel Zakhamoune) is one of the largest identified to date, suggesting that the uppermost Maastrichtian is complete and continuous in both sections. The first biozones identified in the Danian of Sidi Ziane and Djebel Zakhamoune were *G. compressa* (P1c) and *S. triloculinoides* (P1b) Subzones respectively, indicating a hiatus affecting the lower Danian in both sections. Lithologically, this hiatus is only distinguishable by the presence of hardened clayey marls in the uppermost Maastrichtian, so the lower Danian hiatus probably depicts an omission surface and non-depositional unconformity (paraconformity).

Graphic correlation comparing bio- and magnetohorizons from western Tethyan sections, such as Bottaccione (Italy), Agost and Caravaca (Spain), and Kalaat Senan (Aïn Settara and Sidi Nasseur, Tunisia), has enabled to accurately date/calibrate the age of some planktic foraminiferal key-bioevents from the uppermost Maastrichtian to the middle Danian, as well as estimate the durations of planktic foraminiferal zones and subzones. This calibration technique has allowed us to obtain an adequate biochronological control to evaluate the potential for the study of the K/Pg boundary event of the Médéa area. Based on graphic correlation with planktic foraminifera, it has been determined that sedimentation rates in the Maastrichtian of Sidi Ziane and Djebel Zakhamoune are 8.98 cm/kyr and 6.58 cm/kyr respectively, only comparable with the most expanded and continuous sections worldwide, such as Aïn Settara. According to graphic correlation, the lower Danian hiatus has been estimated in 610.4 kyr long in Djebel Zakhamoune and 644.9 kyr long in Sidi Ziane. We speculate that this hiatus may have two origins: 1) an environmental origin, according to which the lower Danian hiatus could be related to changes in the sedimentation/erosion rates during the warming episodes post-K/Pg and Dan-C2; and 2) an tectonic origin, according to which the hiatus could be related to a small tectonic lifting triggered by the K/Pg boundary compressional event that affects the Tellian basin.

The presence of reworked specimens of *Parvularugoglobigerina longiapertura* in Sidi Ziane and Djebel Zakhamoune strongly suggests that the earliest Danian is recorded in the Médéa area, so the search for new nearby sections should be intensified until finding a more continuous section across the K/Pg boundary. In addition, the biostratigraphic data here reported further suggests that the warming episode LMWE of the Late Maastrichtian is well-exposed in this area, at least in Sidi Ziane. Expanding the sampling to earlier levels of the Maastrichtian and conducting multidisciplinary studies (micropaleontological, geochemical and sedimentological) will be necessary to accurately analyze the

LMWE and other climatic episodes of the Late Maastrichtian in the Médéa area, as well as to establish its relationship with the Deccan volcanism.

Acknowledgments

This work was supported by MINECO/FEDER-UE (project number CGL2015-64422-P), by MCIU/AEI/FEDER, UE (grant number PGC2018-093890-B-I00) and by the Departamento de Educación y Ciencia of the Aragonian Government, co-financed by the European Social Fund [grant number DGA group E33_17R]. Vicente Gilabert acknowledges support from the Spanish Ministerio de Economía, Industria y Competitividad (FPI grant BES-2016-077800). The authors would like to acknowledge the use of the Servicio General de Apoyo a la Investigación-SAI, Universidad de Zaragoza.

References

Alvarez LW, Alvarez W, Asaro F, Michel HV (1980) Extraterrestrial cause for the Cretaceous-Tertiary extinction, Science 208:1095–1108

Alvarez W, Arthur MA, Fischer AG, Lowrie W, Napoleone G, Premoli Silva I, Roggenthen WA (1977) Upper Cretaceous-Paleocene magnetic stratigraphy at Gubbio, Italy. V Type section for the Late Cretaceous-Paleocene geomagnetic reversal time scale. Geol Soc Am Bull 88:383–388

Apellaniz E, Baceta JI, Bernaola-Bilbao G, Núñez-Betelu K, Orue-Etxebarria X, Payros A, Pujalte V, Robin E, Rocchia R (1997) Analysis of uppermost Cretaceous-lowermost Tertiary hemipelagic successions in the Basque Country (Western Pyrenees): evidence for a sudden extinction of more than half planktic foraminifer species at the K/T boundary. Bull Soc géol France 168(6):783–793

Arenillas I (1996) Los foraminíferos planctónicos del Paleoceno-Eoceno inferior: Sistemática, Bioestratigrafía, Cronoestratigrafía y Paleoceanografía. Doctoral Thesis, Prensas Universitarias de Zaragoza (2000), Zaragoza, Spain

Arenillas I (1998) Biostratigrafía con foraminíferos planctónicos del Paleoceno y Eoceno inferior de Gubbio (Italia): calibración biomagnetoestratigráfica. Neues Jahrb Geol Paläontol Monatsh 5:299–320

Arenillas I (2011) Análisis paleoecológico de foraminíferos planctónicos del tránsito Daniense-Selandiense en el Tetis y sus implicaciones taxonómicas. Rev Esp Micropalentol 43(1-2):55–108

Arenillas I (2012) Patterns of spatio-temporal distribution as criteria for the separation of planktic foraminiferal species across the Danian-Selandian transition in Spain. Acta Paleontol Polon 57:401–422

Arenillas I, Molina E (1997) Análisis cuantitativo de los foraminíferos planctónicos del Paleoceno de Caravaca (Cordilleras Béticas): Cronoestratigrafía, bioestratigrafía y evolución de las asociaciones. Rev Esp Paleontol 12(2):207–232

Arenillas I, Arz JA (2000) *Parvularugoglobigerina eugubina* type-sample at Ceselli (Italy): planktic foraminiferal assemblage and lowermost Danian biostratigraphic implications. Riv Ital Paleontol Stratigr, 106(3):379–390

Arenillas I, Arz JA (2013a) Origin and evolution of the planktic foraminiferal Family Eoglobigerinidae Blow (1979) in the early Danian (Paleocene). Rev Mex Cienc Geol 30(1):159–177

Arenillas I, Arz JA (2013b) New evidence on the origin of nonspinose pitted-cancellate species of the early Danian planktonic foraminifera. Geol Carpath 64(3):237–251

Arenillas I, Arz JA (2017) Benthic origin and earliest evolution of the first planktonic foraminifera after the Cretaceous/Paleogene boundary mass extinction. Hist Biol 29(1):17–24

Arenillas I, Arz JA, Molina E, Dupuis C (2000a) An independent test of planktic foraminiferal turnover across the Cretaceous/Paleogene (K/P) boundary at El Kef, Tunisia: Catastrophic mass extinction and possible survivorship. Micropaleontology 46(1):31–49

Arenillas I, Arz JA, Molina E, Dupuis C (2000b) The Cretaceous/Paleogene (K/P) boundary at Aïn Settara, Tunisia: sudden catastrophic mass extinction in planktic foraminifera. Jour Foram Res 30(3):202–218

Arenillas I, Arz JA, Molina E (2004) A new high-resolution planktic foraminiferal zonation and subzonation for the lower Danian. Lethaia 37:79–95

Arenillas I, Arz JA, Grajales-Nishimura JM, Murillo-Muñetón G, Alvarez W, Camargo-Zanoguera A, Molina E, Rosales-Domínguez C (2006) Chicxulub impact event is Cretaceous/Paleogene boundary in age: new micropaleontological evidence. Earth Planet Sci Lett, 249:241–257

Arenillas I, Arz JA, Náñez C (2016) New species of genus *Trochoguembelitria* from the lowermost Danian of Tunisia - biostratigraphic and evolutionary implications in planktonic foraminifera. Palaeontograph Abt A 305(4-6):133–160

Arenillas I, Arz JA, Gilabert V (2018) Blooms of aberrant planktic foraminifera across the K/Pg boundary in the Western Tethys: causes and evolutionary implications. Paleobiology 44(3):460-489

Arz JA (1996) Los foraminíferos planctónicos del Campaniense y Maastrichtiense: Bioestratigrafía, Cronoestratigrafía y eventos paleoecológicos. Doctoral Thesis, Prensas Universitarias de Zaragoza (2000), Zaragoza, Spain

Arz JA, Molina E (2002) Bioestratigrafía y cronoestratigrafía con foraminíferos planctónicos del Campaniense superior y Maastrichtiense de latitudes subtropicales y templadas (España, Francia y Tunicia). Neues Jahrb Geol Paläontol Abh 224:161–195

Arz JA, Arenillas I, Molina E, Dupuis C (1999) Los efectos tafonómico y "Signor-Lipps" sobre la extinción en masa de foraminíferos planctónicos en el límite Cretácico/Terciario de Elles (Tunicia). Rev Soc Geol España 12(2):251–268

Arz JA, Arenillas I, Molina E, Sepúlveda R (2000) La estabilidad faunística de foraminíferos planctónicos en el Maastrichtiense superior y su extinción en masa catastrófica en el límite K/T de Caravaca, España. Rev Geol Chile 27(1):27–47

Auboin J, Durand Delga M. (1971) Aire méditerranéenne. Encyclopaedia Universalis 10:743–745

Barnet JSK, Littler K, Kroon D, Leng MJ, Westerhold T, Röhl U, Zachos JC (2017) A new high-resolution chronology for the late Maastrichtian warming event: Establishing robust temporal links with the onset of Deccan volcanism. Geology 46(2):147–150

Birch HS, Coxall, HK, Pearson PN, Kroon D, Schmidt DN (2016) Partial collapse of the marine carbon pump after the Cretaceous-Paleogene boundary. Geology 44:287–290

Berggren WA (1969) Rates of evolution in some Cenozoic planktonic foraminifera. Micropaleontology 15(3):351–365

Berggren WA (1977) Atlas of Paleogene Planktonic Foraminifera. Some species of the genera *Subbotina, Planorotalites, Morozovella, Acarinina* and *Truncorotaloides* Oceanic Micropaleontology, Ramsay, ATS, pp. 250–299

Berggren WA, Miller KG (1988) Paleogene tropical planktonic foraminiferal biostratigraphy and magnetobiochronology. Micropaleontology 34:362–380

Berggren WA, Norris RD (1997) Biostratigraphy, phylogeny and systematics of Paleocene trochospiral planktic foraminifera. Micropaleontology 43:1–116

Berggren WA, Pearson PN (2005) A revised tropical to subtropical Paleogene planktonic foraminiferal zonation. J Foram Res 35:279–298

Berggren WA, Kent DV, Swisher III CC, Aubry MP (1995) A revised Paleogene Geochronology and Chronostratigraphy. In: Berggren WA, Kent DV, Aubry MP, Hardenbol J (eds) Geochronology, time scales and global stratigraphic correlation. SEPM Sp Pub 54:129–213

Blakey RC (2011) Paleogeography of Europe Series. Northern Arizona University, Colorado Plateu Geosystems Inc, Deep Time Maps^{TM}. http://deeptimemaps.com/europe-series-thumbnails/ Accessed 25 July 2007

Blow WH (1969) Late Middle Eocene to Recent planktonic foraminiferal biostratigraphy. In: Brönnimann O, Renz HH (eds), Proceed I Int Conf Plank Microf, 1:199–422

Blow WH (1979) The Cainozoic Globigerinidae. A study of the morphology, taxonomy, evolutionary relationship and the stratigraphical distribution of some Globigerinidae (mainly Globigerinacea). EJ Brill, Leiden

Bolli HM (1957) The genera *Globigerina* and *Globorotalia* in the Paleocene-lower Eocene Lizard Springs formation of Trinidad, B.W.I. US Nat Mus Bull 215:97–124

Bolli HM (1966) Zonation of Cretaceous to Pliocene marine sediments based on Planktonic foraminifera. Bol inf Asoc Venezolana Geol Min Petrol 9(1):1–34

Bouillin JP (1978) La transversale de Collo (Petite Kabylie). Mém Soc géol Fra 135:1-84

Brönnimann P (1952) Globigerinidae from the Upper Cretaceous (Cenomanian–Maastrichtian) of Trinidad. Bull Am Paleontol 34(140):1–30

Canudo JI (1994) *Luterbacheria*: un nuevo género de foraminífero planctónico (Protozoa) del Paleoceno-Eoceno y sus relaciones filogenéticas. Rev Esp Micropaleontol 26(2):23–42

Canudo JI, Molina E (1992) Bioestratigrafía con foraminíferos planctónicos del Paleógeno del Pirineo. Neues Jahrb Geol Paläontol Abh 186:97–135

Canudo JI, Keller J, Molina E (1991) Cretaceous/Tertiary boundary extinction pattern and faunal turnover at Agost and Caravaca, SE Spain. Mar Micropaleontol 17:319–341

Caron M (1985) Cretaceous planktic foraminifera. In Bolli HM, Saunders JB, K. Perch-Nielsen K (eds.), Plankton Stratigraphy, Cambridge University Press

Coccioni R, Premoli-Silva I (2015) Revised Upper Albian – Maastrichtian planktonic foraminiferal biostratigraphy and magneto-stratigraphy of the classical Tethyan Gubbio section (Italy). Newsl Stratigr, 48(1):47-90

Coccioni R, Frontalini F, Bancalà G, Fornaciari E, Jovane L, Sprovieri M (2010) The Dan-C2 hyperthermal event at Gubbio (Italy): Global implications, environmental effects, and cause(s). Earth Planet Sci Lett 297:298–305

Chacón B (2002) Las sucesiones hemipelágicas del final del Cretácico e inicio del Paleógeno en el SE de la Placa Ibérica: Estratigrafía de eventos y evolución de la cuenca. Doctoral Thesis, Universidad Complutense, Madrid, Spain

Chacón B, Martín-Chivelet J (2005) Subdivisión litoestratigráfica de las series hemipelágicas de edad Coniaciense-Thanetiense en el Prebético oriental (SE de España). Rev Soc Geol España 18(1–2):3–20

De Chevilly F., Grégoire, J.-P, Kieken, M. (1961) Carte géologique de l'Algérie 1: 50,000. 111, Souagui. Publ Serv Carte géol, Algérie

Dupuis C, Steurbaut E, Molina E, Rauscher R, Tribovillard NP, Arenillas I, Arz JA, Robaszynski F, Caron M, Robin E, Rocchia R, Lefèvre I (2001) The Cretaceous-Paleogene (K/P) boundary in the Aïn Settara section (Kalaat-Senan, Central Tunisia): lithological, micropaleontological and geochemical evidence. Bull Inst Roy Sci Nat Belgique, 71:169–190

Farouk S (2014) Maastrichtian carbon cycle changes and planktonic foraminiferal bioevents at Gebel Matulla, west-central Sinai, Egypt. Cretaceous Res, 50:238–251

Farouk S (2016) Paleocene stratigraphy in Egypt. J Afr Earth Sci, 113:126–152

Farouk S, Jain S (2018) Benthic foraminiferal response to relative sea-level changes in the Maastrichtian-Danian succession at the Dakhla Oasis, Western Desert, Egypt. Geol Mag, 155(3):729–746

Farouk S, Marzouk AM, Fayez A (2014) The Cretaceous / Paleogene boundary in Jordan. J Asian Earth Sci, 94:113–125

Galeotti S, Moretti M, Cappelli C, Phillips J, Lanci L, Littler K, Monechi S, Petrizzo MR, Premoli Silva I, Zachos JC (2015) The Bottaccione Section at Gubbio, Central Italy: A Classic Palaeocene Tethyan Setting Revisited. Newsl Stratigr 48(3):325–339

Gallala N (2013) Planktonic Foraminiferal Biostratigraphy and Correlation Across the Cretaceous-Paleogene Transition at the Tethyan and the Atlantic Realms. Paleontol J 2013:1–20

Gardin S, Galbrun B, Thibault N, Coccioni R, Premoli Silva I (2012) Bio-magnetochronology for the upper Campanian – Maastrichtian from the Gubbio area, Italy: new results from the Contessa Highway and Bottaccione sections. Newsl Stratigr 45(1):75–103

Guiraud R (1998) Mesozoic rifting and basin inversion along the northern African Tethyan margin: an overview. Geol Soc London Spec Publ 133: 217–229

Guiraud, R., Bosworth, W (1997) Senonian basin inversion and rejuvenation of rifting in Africa and Arabia: synthesis and implications to plate-scale tectonics. Tectonophysics 282, 39–82

Guiraud R, Bosworth W, Thierry J, Delplanque A (2005) Phanerozoic geological evolution of Northern and Central Africa: An overview. J Afr Earth Sci 43:83–143

Gradstein FM, Ogg JG, Schmitz M, Ogg G (2012) The Geologic Time Scale 2012, Elsevier, Amsterdam

Groot JJ, De Jonge RBG, Langereis CG, Ten Kate WGHZ, Smit J (1989) Magnetostratigraphy of the Cretaceous-Tertiary boundary at Agost (Spain). Earth Plan Sci Lett 94:385–397

Hildebrand AR, Penfield GT, Kring DA, Pilkington M, Camargo A, Jacobsen SB, Boynton WV (1991) Chicxulub crater: A possible Cretaceous/Tertiary boundary impact crater on the Yucatan peninsula, Mexico. Geology 19:867–871

Huber BT, MacLeod KG, Tur NA (2008) Chronostratigraphic framework for upper Campanian–Maastrichtian sediments on the Blake Nose (Subtropical North Atlantic). J Foraminiferal Res 38:162–182

Ion J, Szasz L (1994) Biostratigraphy of the Upper Cretaceous in Romania. Cret Res 15:59–87

Kaiho K, Kajiwara Y, Tazaki K, Ueshima M, Takeda N, Kawahata H, Arinobu T, Ishiwatari R, Hirai A, Lamolda MA (1999) Oceanic primary productivity and dissolved oxygen levels at the Cretaceous/Tertiary Boundary: Their decrease, subsequent warming, and recovery. Paleoceanography 14(4): 511–524

Keller G (1988) Extinction, survivorship and evolution of planktic foraminifera across the Cretaceous/Tertiary boundary at El Kef, Tunisia. Mar Micropaleontol 13:239–263

Keller G (1993) The Cretaceous/Tertiary boundary transitions in the Antarctic Ocean and its global implications. Mar Micropaleont 21:1–45

Keller G, Lindinger M (1989) Stable isotope, TOC and $CaCO_3$, record across the Cretaceous/Tertiary boundary at El Kef, Tunisia. Palaeogeogr Palaeoclimatol Palaeoecol 73:243–265

Keller G, Li L, MacLeod N (1995) The Cretaceous/Tertiary boundary stratotype sections at El Kef, Tunisia: How catastrophic was the mass extinction?. Palaeogeogr Palaeoclimatol Palaeoecol 119:221–254

Keller G, Bhowmick PH, Upadhyay H, Dave A, Reddy AN, Jaiprakash BC, Adatte T (2011) Deccan volcanism linked to the Cretaceous-Tertiary Boundary mass extinction: New evidence from ONGC wells in the Krishna-Godavari basin. J Geol Soc India 78:399–428

Keller G, Mateo P, J. Punekar J (2016) Upheavals during the Late Maastrichtian: Volcanism, climate and faunal events preceding the end-Cretaceous mass extinction. Palaeogeogr Palaeoclimatol Palaeoecol 441:137–151

Kieken M (1963) Notice de la carte géologique à 1/50 000 (levés de F. De Chevilly, J.Y. Grégoire). Publ Serv Carte Géol, Algérie

Kieken M (1974) Etude géologique du Hodna, du Titteri et de la partie occidentale des Biban (Dépt. D'Alger-Algérie). Thèse de Doctorat es-Sciences, Alger, Service géologique de l'Algérie

Leonov GP, Alimarina VP (1961) Stratigraphy and foraminifera of Cretaceous-Paleogene "transition" beds of the central part of the North Caucasus. Moscow Univ Geol Faculty, sbornik Trudov, 29–60

Li L, Keller, G (1998) Abrupt deep-sea warming at the end of the Cretaceous. Geology 26:995–998

Lowrie W, Alvarez W, Napoleone G, Perch Nielsen K, Premoli Silva I, Toumarkine M (1982) Paleogene magnetic stratigraphy in Umbrian pelagic carbonate rocks: The Contessa sections, Gubbio. Geol Soc Am Bull, 93:414–432

Luterbacher HP (1964) Studies in some *Globorotalia* from the Paleocene and lower Eocene of the central Apennines. Eclogae geol Helvet 57(2):631–730

Luterbacher HP (1975) Planktonic foraminifera of the Paleocene and early Eocene, Possagno section. Schweiz Paläontol Abh 97:57–67

Luterbacher HP, Premoli Silva I (1964) Biostratigrafia del limite Cretaceo-Terziario nell´Apennino Centrale. Riv Ital Paleontol Stratigr 70(1):67–128

Martínez-Ruiz F, Ortega-Huertas M, Palomo-Delgado I, Barbieri, M (1992) The geochemistry and mineralogy of the Cretaceous-Tertiary boundary at Agost (southeast Spain). Chem Geol 95:265–281

Martínez-Ruiz F, Ortega-Huertas M, Palomo-Delgado I, Acquafredda P (1997) Quench textures in altered spherules from the Cretaceous-Tertiary boundary layer at Agost and Caravaca, SE Spain. Sediment Geol 113:137–147

Molina E, Arenillas I, Arz JA (1996) The Cretaceous/Tertiary boundary mass extinction in planktic foraminifera at Agost (Spain). Rev Micropaléontol 39(3):225–243

Molina E, Arenillas I, Arz JA (1998) Mass extinction in planktic foraminifera at the Cretaceous/Tertiary boundary in subtropical and temperate latitudes. Bull Soc géol France 169(3):351–363

Molina E, Alegret L, Arenillas I, Arz JA (2005) The Cretaceous/Paleogene boundary at the Agost section revisited: paleoenvironmental reconstruction and mass extinction pattern. J Iberian Geol 31:137–150

Molina E, Alegret L, Arenillas I, Arz JA, Gallala N, Hardenbol J, von Salis K, Steurbaut E, Vandenberghe N, Zaghbib-Turki D (2006) The Global Stratotype Section and Point of the Danian Stage (Paleocene, Paleogene, "Tertiary", Cenozoic) at El Kef, Tunisia: original definition and revision. Episodes 29(4):263–278

Molina E, Alegret L, Arenillas I, Arz JA, Gallala N, Grajales-Nishimura M, Murillo-Muñetón G, Zaghbib-Turki D (2009) The Global Boundary Stratotype Section and Point for the base of the Danian Stage (Paleocene, Paleogene, "Tertiary", Cenozoic): auxiliary sections and correlation. Episodes 32(2):84–95

Montanari A (1991) Authigenesis of impact spheroids in the K/T boundary clay from Italy: New constraints for high-resolution stratigraphy of terminal Cretaceous events. J Sed Petrol 61(3):315–339

Morozova VG (1957) Nadsemeystvo foraminifer Globigirinidea superfam. nova i nekotorye ego predstaviteli [Foraminiferal superfamily Globigerinidea superfam. nov., and some of its representatives]. Doklady Akad. Nauk SSSR, 114:1109–1112

Mukhopadhyay S, Farley KA, Montanari A (2001) A short duration of the Cretaceous-Tertiary boundary event: Evidence from extraterrestrial Helium-3. Science 291:1952–1955

Nederbragt AJ (1990) Biostratigraphy and paleoceanographic potential of the Cretaceous planktic foraminifera Heterohelicidae. Academisch proefschrift, Centrale Huisdrukkerij Vrije Universiteit, Amsterdam

Nederbragt AJ (1991) Late Cretaceous biostratigraphy and development of Heterohelicidae (planktic foraminifera). Micropaleontology 37:329–372

Olsson RK, Hemleben C, Berggren WA, Liu C (1992) Wall texture classification of planktonic foraminifera genera in the Lower Danian. J Foramin Res 22(3):195–213

Olsson RK, Hemleben C, Berggren WA, Huber BT (1999) Atlas of Paleocene Planktonic Foraminifera. Smithsonian Contrib Paleobiol 85:1–252

Quillévéré F, Norris RD, Kroon D, Wilson PA (2008) Transient ocean warming and shifts in carbon reservoirs during the early Danian. Earth Planet Sci Lett 265:600–615

Pérez-Rodríguez I, Lees JA, Larrasoaña JC, Arz, JA, Arenillas I (2012) Planktonic foraminiferal–nannofossil biostratigraphy and magnetostratigraphy of the uppermost Campanian and Maastrichtian at Zumaia, northern Spain. Cretaceous Res 37:100–126

Petersen SV, Dutton A, Lohmann KC (2016) End-Cretaceous extinction in Antarctica linked to both Deccan volcanism and meteorite impact via climate change. Nat Commun 7:12079

Punekar J, Mateo P, Keller G (2014) Effects of Deccan volcanism on paleoenvironment and planktic foraminifera: A global survey. GSA Spec Pap 505:91–116

Punekar J, Keller G, Khozyem HM, Adatte T, Font E, Spangnberg J (2016) A multi-proxy approach to decode the end-Cretaceous mass extinction. Palaeogeogr Palaeoclimatol Palaeoecol 441:116–136

Premoli Silva I, Sliter WV (1995) Cretaceous planktonic foraminiferal biostratigraphy and evolutionary trends from the Bottaccione section, Gubbio, Italy. Paleontographia Italica 82:1–89

Premoli Silva I, Paggi L, Monechi S (1976) Cretaceous through Paleocene biostratigraphy of the pelagic sequence at Gubbio, Italy. Mem Soc Geol It 2:21–32

Premoli Silva I, Napoleone G, Fischer A (1980) La sezione magnetostratigrafica di Gubbio: indagini nella storia del Cretacico-Paleogene. Mem Soc Geol It 21:301–311

Renne PR, Sprain CJ, Richards MA, Self S, Vanderkluysen L, Pande K (2015) State shift in Deccan volcanism at the Cretaceous-Paleogene boundary, possibly induced by impact. Science 350:76–78

Richards MA, Alvarez W, Self S, Karlstrom L, Renne PR, Manga M, Sprain CJ, Smit J, Vanderkluysen L, Gibson SA (2015) Triggering of the largest Deccan eruptions by the Chicxulub impact. GSA Bulletin 127:1507–1520

Robaszynski F, Caron M (1995) Foraminifères planctoniques du Crétacé: Commentaire de la zonation Europe-Méditerranée. Bull Soc géol France 166(6):681–692

Robaszynski F, Caron M, González-Donoso JM, Wonders, AAH (1983-1984) Atlas of Late Cretaceous globotruncanids. Rev Micropal 26(3-4):1–305

Scotese CR (2014) Atlas of Late Cretaceous Paleogeographic Maps. PALEOMAP Atlas for ArcGIS (PALEOMAP Project, Evanstan, IL), 2: map 16

Schoene B, Samperton KM, Eddy MP, Keller G, Adatte T, Bowring SA, Khadri SFR, Gertsch B (2015) U-Pb geochronology of the Deccan Traps and relation to the end-Cretaceous mass extinction. Science 347:182–184

Shaw AB (1964) Time in stratigraphy. McGraw-Hill, New York, NY

Smit J (1982) Extinction and evolution of planktonic foraminifera after a major impact at the Cretaceous/Tertiary boundary. Geol Soc Am Spec Pap 190:329–352

Smit J (1999) The global stratigraphy of the Cretaceous-Tertiary boundary impact ejecta. Ann Rev Earth Pl Sci 27:75–113

Smit J (2004) The section of the Barranco del Gredero (Caravaca, SE Spain): a crucial section for the Cretaceous/Tertiary boundary impact extinction hypothesis. J Iberian Geol 31:179–191

Smit J, Hertogen J (1980) An extraterrestrial event at the Cretaceous-Tertiary boundary. Nature 285:198–200

Sprain CJ, Renne PR, Clemens WA, Wilson GP (2018) Calibration of chron C29r: New high-precision geochronologic and paleomagnetic constraints from the Hell Creek region, Montana. GSA Bull, doi: 10.1130/B31890.1

Stainforth RM, Lamb JL, Luterbacher H, Beardand JH, Jeffords RM (1975) Cenozoic planktonic foraminifera1 zonation and characteristics of index form. Univ Kansas Paleont Contr Art 62:l–425

Steurbaut, E., Dupuis, C., Arenillas, I., Molina, E., Matmati, MF (2000) The Kalaat Senan section in Central Tunisia: A potencial reference section for the Danian/Selandian boundary. GFF 122(1):158–160

Thibault N, Galbrun B, Gardin S, Minoletti F, Le Callonnec LL (2016) The end-Cretaceous in the southwestern Tethys (Elles, Tunisia): orbital calibration of paleoenvironmental events before the mass extinction. Int J Earth Sci (Geol Rundschau) 105:771–795

Toumarkine M, Luterbacher HP (1985) Paleocene and Eocene planktic foraminifera. In Bolli HM, Saunders JB, Perch-Nielsen K (eds), Plankton Stratigraphy. Cambridge University Press

van Veen, GW (1969) Geological investigations in the region west of Caravaca, south-eastern Spain. University dissertation, Amsterdam University, Netherlands

Vera JA, García-Hernández M, López Garrido AC, Comas MJ, Ruíz-Ortíz PA, Martín-Algarra A (1982) La Cordillera Bética. In: García A (chief coordinator) El Cretácico de España, Editorial Univ Complutense, Madrid, Spain

Wade BR, Pearson PN, Berggren WA, Pälike H (2011) Review and revision of Cenozoic tropical planktonic foraminiferal biostratigraphy and calibration to the geomagnetic polarity and astronomical time scale. Earth-Sci Rev 104:111–142

Wildi W (1983) La chaîne tello rifaine (Algérie, Maroc, Tunisie): structure, stratigraphie et évolution du Trias au Miocène. Rev Géol Dyn Géogr Phys 24(3):201–297

Appendix 1. Taxonomic remarks

Diagnostic characters of the most relevant Maastrichtian species

(1) *Abathomphalus mayaroensis* (Bolli 1951): Trochospiral test, with flat to slightly convex spiral side and flat to slightly concave umbilical side, 4½ - 5½ crescent-moon box shaped chambers in the last whorl, moderate rate of chamber size increase, axial periphery truncated and limited by two marginal carinas, primary aperture umbilical, coverplate covering the umbilicus with several secondary apertures, wall texture pitted with pustules or rugosities usually aligned (Figs. 6.1, 8.1, 9.1).

(2) *Pseudoguembelina hariaensis* Nederbragt 1991: Biserial test, initially rapidly flaring, with final multiserial stage, laterally elongated globular chamber in biserial stage and compressed chamberlets in multiserial stage, apertures high and narrow arcs, bordered by small flanges, wall texture finely costulate (striate) (Figs. 6.2, 8.2, 9.2).

(3) *Plummerita hantkeninoides* (Bronnimann 1952): Trochospiral test, with low spire, 5 - 6 radially elongate chambers with axially situated spines in the last whorl, moderate rate of chamber size increase, aperture umbilical, lip thick, wall texture rugose, many times with a linear pattern (Figs. 6.3, 8.3, 9.3).

(4) *Archaeoglobigerina cretacea* (d'Orbigny, 1840): Trochospiral test, with low spire, 5 - 6 subglobular chambers in the last whorl, low rate of chamber size increase, axial periphery rounded or slightly truncated, with imperforate band and occasionally with two (murico-)carina very poorly developed, aperture umbilical with tegilla, wall texture rugose (Figs. 6.4, 8.4, 9.4).

(5) *Muricohedbergella holmdelensis* (Olsson 1964): Trochospiral test, 5 - 6½ moderately compressed hemispherical to subconical chambers in the last whorl, low rate of chamber size increase, axial periphery slightly angular, aperture umbilical-extraumbilical, with lip thick, wall texture pustulate to muricate (Figs. 6.5, 8.5, 9.5).

(6) *Guembelitria cretacea* Cushman 1933: Small triserial test, globular chambers, moderate rate of chamber size increase, umbilical aperture, wide arch, with lip thin, wall texture pore-mounded (Figs. 6.6, 8.6, 9.6).

Diagnostic characters of the most relevant Danian species

Parvularugoglobigerinid lineage

(1) *Parvularugoglobigerina longiapertura* (Blow 1979): Small trochospiral test, with low spire, 5 - 6½ slightly to moderately compressed ovate chambers in the last whorl, low rate of chamber size increase, umbilical-extraumbilical aperture extending up into the apertural chamber face, high and narrow arch, with lip thin, wall texture smooth, microperforate (Fig. 6.7, 8.7).
(2) *Parvularugoglobigerina eugubina* (Luterbacher & Premoli Silva 1964): Small trochospiral test, with low spire, 5 - 6½ globular chambers in the last whorl, low rate of chamber size increase, aperture umbilical-extraumbilical, low arch, with lip thin, wall texture smooth, microperforate (Fig. 6.8).
(3) *Parvularugoglobigerina sabina* (Luterbacher & Premoli Silva 1964): Small trochospiral test, with slightly high spire, 4½ - 5 globular chambers in the last whorl, moderate rate of chamber size increase, aperture umbilical to somewhat extraumbilical, low arch, with lip thin, wall texture smooth, microperforate (Fig. 6.9).

Eoglobigerinid lineage

(4) *Eoglobigerina simplicissima* Blow (1979): Trochospiral test, with low spire, 3½ - 4 subglobular chambers in the last whorl, low to moderate rate of chamber size increase, aperture umbilical, lip moderately thick, wall texture weakly cancellate, spinose (Figs. 6.10).
(5) *Eoglobigerina eobulloides* Morozova (1959): Trochospiral test, with low spire, 4 - 4½ subglobular chambers in the last whorl, low rate of chamber size increase, aperture umbilical to somewhat extraumbilical, lip moderately thick, wall texture cancellate, spinose (Figs. 6.11).

(6) *Eoglobigerina* cf. *trivialis* (*E. trivialis* Subbotina 1953, sensu Blow 1979): Trochospiral test, with lightly high spire, 3 ½ - 4 spherical chambers in the last whorl, low to moderate rate of chamber size increase, aperture umbilical, lip moderately thick, wall texture cancellate, spinose (Figs. 6.12, 8.8, 9.7).
(7) *Parasubbotina pseudobulloides* (Plummer 1927): Trochospiral test, with low spire, 4½ - 5 subglobular chambers in the last spiral whorl, moderate rate of chamber size increase, aperture umbilical-extraumbilical, lip moderately thick, wall texture cancellate, spinose (Figs. 6.14, 8.9, 9.8).
(8) *Subbotina triloculinoides* (Plummer 1927): Trochospiral test, with low spire, 3 - 3½ subglobular chambers in the last whorl, moderate to high rate of chamber size increase, aperture umbilical to somewhat extraumbilical, lip thick, wall texture cancellate, spinose (Figs. 6.13, 8.11, 9.9).

Praemurica-Acarinina lineage

(9) *Praemurica taurica* (Morozova 1961): Trochospiral test, with low to flat spire, 5½ - 7 subglobular chambers in the last whorl, low rate of chamber size increase, aperture umbilical-extraumbilical, with lip thick, wall surface cancellate (Figs. 6.15, 8.12, 9.10).
(10) *Praemurica pseudoinconstans* (Blow 1979): Trochospiral test, with low to flat spire, 5 - 5½ subglobular chambers in the last whorl, initially with low rate of chamber size increase and finally moderate to high rate (last inflated chambers), sutures straight or slightly curved on the spiral side, aperture umbilical-extraumbilical, with lip thick, wall texture cancellate (Figs. 6.16, 8.14, 9.11).
(11) *Praemurica inconstans* (Subbotina 1953): Trochospiral test, with low to flat spire, 5 - 6½ inflated subglobular chambers in the last whorl, moderate rate of chamber size increase, sutures straight or slightly curved on the spiral side, aperture umbilical-extraumbilical, with lip thick, wall texture cancellate (Figs. 6.20, 8.16-17, 9.13).
(12) *Acarinina trinidadensis* (Bolli 1957): Trochospiral test, with low spire, 5 - 7 chambers in the last whorl initially hemisphaerical and finally globular, low to moderate rate of chamber size increase, sutures initially curved and finally straight or slightly curved, aperture umbilical-extraumbilical, lip moderately thick, wall texture initially muricate and finally cancellate (Figs. 21, 8.18, 9.15).
(13) *Acarinina uncinata* (Bolli 1957): Trochospiral test, with low spire, 5 - 6 hemisphaerical chambers in the last whorl, low to moderate rate of chamber size increase, sutures curved (or slightly curved in the last

chambers), aperture umbilical-extraumbilical, lip moderately thick, wall texture muricate (Figs. 6.22, 8.19, 9.16).

(14) *Acarinina praecursoria* Morozova (1957): Trochospiral test, discoidal and lobate, with low spire, 6½ - 8 hemisphaerical chambers in the last whorl, low rate of chamber size increase, sutures curved (or slightly curved in the last chambers), aperture umbilical-extraumbilical, lip moderately thick, wall texture muricate (Figs. 6.23).

Globanomalina-Luterbacheria lineage

(15) *Globanomalina compressa* (Plummer 1927): Trochospiral test, biconvex, 4½ - 5½ slightly to moderately compressed ovate chambers in the last whorl, low to moderate rate of chamber size increase, axial periphery slightly to moderately angular, with imperforate band usually little developed or absent, aperture umbilical-extraumbilical, with lip thick, wall texture pitted (Figs. 6.17, 8.10, 9. 12).

(16) *Globanomalina haunsbergensis* (Gohrbandt 1963): Trochospiral test, biconvex, 4½ - 6 moderately to strongly compressed ovate chambers in the last whorl, low to moderate rate of chamber size increase, axial periphery moderately to strongly angular, with imperforate band well developed, aperture umbilical-extraumbilical, with lip thick, wall texture pitted (Figs. 6.18, 8.13, 9.14).

(17) *Luterbacheria ehrenbergi* (Bolli 1957): Trochospiral test, compressed biconvex, 5 - 6 strongly compressed ovate chambers in the last whorl, low to moderate rate of chamber size increase, axial periphery moderately to strongly angular, with carina partially or poorly developed, aperture umbilical-extraumbilical, with lip thick, wall texture pitted (Figs. 6.19, 8.15).

Figure Captions

Fig. 1 Geographical locations (a) and geological maps (b, c) showing the Cretaceous/Paleogene boundary sections studied in the explored Médéa area, Algeria. Geological maps modified after De Chevilly (1961) and Kieken (1963, 1974). SZ = Sidi Ziane section; DZ = Djebel Zakhamoune section.

Fig. 2 Field overviews of the Sidi Ziane (a) and Djebel Zakhamoune (b) sections. K = Cretaceous; Pg = Paleogene.

Fig. 3 Stratigraphy and lithostratigraphic correlation of Sidi Ziane and Djebel Zakhamoune sections. The lithostratigraphic Unit I was defined by Kieken (1974). Lithozones A_D and A_M = lithofacies A in Danian and Maastrichtian, predominantly consisting of clayey marls; Lithozones B_D and B_M = lithofacies A in Danian and Maastrichtian, consisting of intercalations of marly limestones and marls; Lithozone C = lithofacies C, consisting of hardened dark clayey marls.

Fig. 4 Locations of analyzed sections of Médea, Kalaan Senan, Bottaccione, Agost and Caravaca, plotted on a paleogeographic reconstruction of Tethys at the time of the K/Pg boundary. Source of paleogeographic setting at http://legacy.earlham.edu/~riethju/stuff/latecretmed.jpg, modified according to Guiraud et al. (2005), Blakey (2011) and Scotese (2014).

Fig. 5 Correlation of the main planktic foraminiferal zonations of the Cretaceous-Paleogene transition with the magnetostratigraphic scale, and bio-chronostratigraphic ranges of the most revelant planktic foraminiferal species, including index-species. Age of paleomagnetic reversals and K/Pg boundary based on Geological Time Scale GTS2012 (Gradstein et al. 2012). (1) Biozonation described in this report, based on Arz and Molina (2002) for the Maastrichtian, and Arenillas and Molina (1997) and Arenillas et al. (2004) for the Danian. (2) Biozonation of Berggren and Pearson (2005) for the Danian. (3) Biozonation of Li and Keller (1998) for the Maastrichtian, and Keller (1988, 1993) and Keller et al. (1995) for the Danian. (4) Biozonation of Smit (1982) for the Maastrichtian-Danian transition. Dashed and diagonal lines in biozonal boundaries are due to discrepancies in taxonomy, species ranges and bio-magnetostratigraphic correlations (see text).

Fig. 6 Plate of SEM-photos of the most relevant planktic foraminiferal species of the upper Maastrichtian and Danian (scale bar = 100 microns). 1. *Ab. mayaroensis*, from the Zone CF2, Aïn Settara; 2. *Pg. hariaensis*, from the Zone CF1, Aïn Settara; 3. *Pt. hantkeninoides*, from the Zone CF1, Aïn Settara; 4. *A. cretacea*, from the Zone CF2, Aïn Settara; 5. *Mh. holmdelensis*, from the *Pv. longiapertura* Subzone, Aïn Settara; 6. *Gb. cretacea*, from the Zone CF1, Aïn Settara; 7. *Pv. longiapertura*, from the *Pv. sabina* Subzone, Aïn Settara; 8. *Pv. eugubina*, from the *E. simplicissima* Subzone, Aïn Settara; 9. *Pv. sabina*, from the *E. simplicissima* Subzone, Agost; 10. *E. simplicissima*, from the *E. simplicissima* Subzone, Aïn Settara; 11. *E. eobulloides*, from the *E. simplicissima* Subzone, Aïn Settara; 12. *E.* cf. *trivialis*, Aïn Settara, from the *S. triloculinoides* Subzone, Aïn Settara; 13. *S. triloculinoides*, from the *Ac. uncinata* Subzone, Sidi Nasseur; 14. *P. pseudobulloides*, from the *Ac. uncinata* Subzone, Sidi Nasseur; 15. *Pr. taurica*, from *Ac. uncinata* Subzone, Sidi Nasseur; 16. *Pr. pseudoinconstans*, from the *G. compressa* Subzone, Aïn Settara; 17. *G. compressa*, from the *Ac. uncinata* Zone, Sidi Nasseur; 18. *G. haunsbergensis*, from the *Ac. uncinata* Zone, Sidi Nasseur; 19. *L. ehrenbergi*, from the *Ac. uncinata* Zone, Sidi Nasseur; 20. *Pr. inconstans*, from the *Ac. uncinata* Zone, Sidi Nasseur; 21. *Ac. trinidadensis*, from the *Ac. uncinata* Zone, Sidi Nasseur; 22. *Ac. uncinata*, from the *Ac. uncinata* Zone, Sidi Nasseur; 23. *Ac. praecursoria*, from the *Ac. uncinata* Zone, Agost.

Fig. 7 Biostratigraphic correlation of Sidi Ziane and Djebel Zakhamoune sections and stratigraphic ranges of the most revelants species in both sections. Dashed lines indicate ranges based on reworked specimens.

Fig. 8 Plate of SEM-photos of the most relevant planktic foraminiferal species in Sidi Ziane (scale bar = 100 microns). 1. *Ab. mayaroensis*, from the Zone CF1; 2. *Pg. hariaensis*, from the Zone CF2; 3. *Pt. hantkeninoides*, from the Zone CF1; 4. *A. cretacea*, from the Zone CF1; 5. *Mh. holmdelensis*, from the Zone CF1; 6. *Gb. cretacea*, from the Zone CF1Zone; 7. *Pv. longiapertura*, reworked specimen from the *G. compressa* Subzone; 8. *E.* cf. *trivialis*, from the *Ac. trinidadensis* Zone; 9. *P. pseudobulloides*, from the *G. compressa* Subzone; 10. *G. compressa*, from the *G. compressa* Subzone; 11. *S. triloculinoides*, from the *G. compressa* Subzone; 12. *Pr. taurica*, from the *G. compressa* Subzone; 13. *G. haunsbergensis*, from the *Ac. uncinata* Zone; 14. *Pr. pseudoinconstans*, from the *Ac. trinidadensis* Zone; 15. *L. ehrenbergi*, from the *Ac. uncinata* Zone; 16. *Pr. inconstans*, from the *G. compressa* Subzone; 17. *Pr.*

inconstans, from the *Ac. trinidadensis* Zone; 18. *Ac. trinidadensis*, from the *Ac. trinidadensis* Zone; 19. *Ac. uncinata*, from the *Ac. uncinata* Zone.

Fig. 9 Plate of SEM-photos of the most relevant planktic foraminiferal species - Danian in Djebel Zakhamoune (scale bar = 100 microns). 1. *Ab. mayaroensis*, from the Zone CF1; 2. *Pg. hariaensis*, from the Zone CF2; 3. *Pt. hantkeninoides*, from the Zone CF1; 4. *A. cretacea*, from the Zone CF2; 5. *Mh. holmdelensis*, from the Zone CF2; 6. *Gb. cretacea*, from the Zone CF1; 7. *E.* cf. *trivialis*, from the *S. triloculinoides* Subzone; 8. *P. pseudobulloides*, from the *G. compressa* Subzone; 9. *S. triloculinoides*, from the *Ac. trinidadensis* Zone; 10. *Pr. taurica*, from the *Ac. trinidadensis* Zone; 11. *Pr. pseudoinconstans*, from the *S. triloculinoides* Subzone; 12. *G. compressa*, from the *Ac. trinidadensis* Zone; 13. *Pr. inconstans*, from the *Ac. trinidadensis* Zone; 14. *G. haunsbergensis*, from the *Ac. trinidadensis* Zone; 15. *Ac. trinidadensis*, from the *Ac. trinidadensis* Zone; 16. *Ac. uncinata*, from the *Ac. uncinata* Zone.

Fig. 10 Bio-magnetostratigraphic correlation of Bottaccione, Agost, Caravaca and Kalaat Senan (Aïn Settara + Sidi Nasseur). (1) Biostratigraphic scales: In Bottaccione, based on Arenillas (1998) for the Danian and Coccioni and Premoli Silva (2015) for the Maastrichtian; in Agost, based on Arz (1996), Arenillas (1996), Molina et al. (1996, 1998, 2005), and Arenillas et al. (2005); in Caravaca, based on Arz (1996), Arenillas (1996), Arenillas and Molina (1997) and Arz et al. (2000); in Kalaat Senan, based on Arz (1996), Arenillas (1996), Steurbaut et al. (2000) and Arenillas et al. (2000b). (2) Magnetostratigraphic scales: In Bottaccione, based on Alvarez et al. (1977), Premoli Silva et al. (1980), Lowrie et al. (1982) and Coccioni and Premoli Silva (2015); in Agost, based on Groot et al. (1989); in Caravaca, based on Smit (1982). CF2 = *Pseudoguembelina palpebra* Zone o upper part of *Pseudoguembelina hariaensis* Zone; CF1 = *Plummerita hantkeninoides* Zone; (A) = *Guembelitria cretacea* and *Parvularugoglobigerina eugubina* Zones, and *Eoglobigerina trivialis* Subzone; S.t. = *Subbotina triloculinoides* Subzone; G.c. = *Globanomalina compressa* Subzone; A.t. = *Acarinina trinidadensis* Zone; A.u. = *Acarinina uncinata* Zone.

Fig. 11 Graphic correlation for calibration/datation of planktic foraminiferal data/events of the K-Pg transition based on bio-magnetostratigraphic reference points from Bottacione and Caravaca (see Table

1). (-3) HOD of *Gansserina gansseri*; (-2) LOD of *Plummerita hantkeninoides*; (-1) HOD of *Archaeoglobigerina cretacea*; (+5) LOD of *Subbotina triloculinoides*; (+6) LOD of *Globanomalina compressa*; (+7) LOD of *Acarinina trinidadensis*; (+8) LOD of *Globanomalina haunsbergensis*; (+9) LOD of *Acarinina uncinata*; (+10) LOD of *Luterbacheria ehrenbergi*. Correlation black points = paleomagnetic reversals and K/Pg boundary.

Fig. 12 Graphic correlation for calibration/datation of planktic foraminiferal data/events of the earliest Danian based on bio-magnetostratigraphic reference points from Agost and Caravaca (see Table 1). (+1) LOD of *Parvularugoglobigerina longiapertura*; (+2) LOD of *Parvularugoglobigerina eugubina*; (+3) LOD of *Eoglobigerina simplicissima*; (+4) LOD of *Parasubbotina pseudobulloides*; (+5) LOD of *Subbotina triloculinoides*; (a) Change of sedimentation rate in Caravaca with respect to Agost. (a) Inflection point in sedimentation rate at Caravaca with respect to the selected Standard Reference Section (SRS) of Agost. Correlation black points = paleomagnetic reversals and K/Pg boundary.

Fig. 13 Graphic correlation for the K-Pg transition of Kalaat Senan (Aïn Settara + Sidi Nasseur) and for the lower Danian of Aïn Settara (see Table 2). (-2) LOD of *Plummerita hantkeninoides*; (-1) HOD of *Archaeoglobigerina cretacea*; (+1) LOD of *Parvularugoglobigerina longiapertura*; (+2) LOD of *Parvularugoglobigerina eugubina*; (+3) LOD of *Eoglobigerina simplicissima*; (+4) LOD of *Parasubbotina pseudobulloides*; (+5) LOD of *Subbotina triloculinoides*; (+6) LOD of *Globanomalina compressa*; (+7) LOD of *Acarinina trinidadensis*; (+8) LOD of *Globanomalina haunsbergensis*; (+9) LOD of *Acarinina uncinata*; (+10) LOD of *Luterbacheria ehrenbergi*.

Fig. 14 Graphic correlation for the K-Pg transition of Djebel Zakhamoune (see Table 2). (-2) LOD of *Plummerita hantkeninoides*; (-1) HOD of *Archaeoglobigerina cretacea*; (+5) LOD of *Subbotina triloculinoides*; (+6) LOD of *Globanomalina compressa*; (+7) LOD of *Acarinina trinidadensis*; (+8) LOD of *Globanomalina haunsbergensis*; (+9) LOD of *Acarinina uncinata*; (+10) LOD of *Luterbacheria ehrenbergi*. (A_{D1}) Base of lithozone A_{D1}.

Fig. 15 Graphic correlation for the K-Pg transition of Sidi Ziane (see Table 2). (-2) LOD of *Plummerita hantkeninoides*; (-1) HOD of *Archaeoglobigerina cretacea*; (+5) LOD of *Subbotina triloculinoides*; (+6)

LOD of *Globanomalina compressa*; (+7) LOD of *Acarinina trinidadensis*; (+8) LOD of *Globanomalina haunsbergensis*; (+9) LOD of *Acarinina uncinata*; (+10) LOD of *Luterbacheria ehrenbergi*. (A_{D1}) Base of lithozone A_{D1}.

Table 1 Magneto- and biostratigraphic data from Bottaccione, Agost and Caravaca for the graphic correlations, calculation of sedimentation rates and calibration/datation of planktic foraminiferal data/events (see references in text). Planktic foraminiferal biostratigraphic data based on Arz (1996), Arenillas (1996, 1998), Molina et al. (1996, 1998, 2005, 2009), Arenillas and Molina (1997), Arz et al. (2000), Steurbaut et al. (2000), Arenillas et al. (2004) and Coccioni and Premoli Silva (2015). Paleomagnetic data based on Alvarez et al. (1977), Premoli Silva et al. (1980), Smit (1982), Lowrie et al. (1982), Groot et al. (1989) and Coccioni and Premoli Silva (2015). LOD and HOD = Lowest and Highest Occurrence Datum; FA and LA = First and Last Appearance.

Table 2 Biostratigraphic data from Kalaat Senan (Aïn Settara + Sidi Nasseur) for the graphic correlations and calculation of sedimentation rates. Planktic foraminiferal data based on Arz (1996), Arenillas (1996), Steurbaut et al. (2000), Dupuis et al. (2001), Arenillas et al. (2000b, 2004) and Molina et al. (2009).

Table 3 Biostratigraphic data from Sidi Ziane and Djebel Zakhamoune for the graphic correlations and calculation of sedimentation rates. * Estimated age for the base of interval A_{D1}, according to sedimentation rate of the *G. compressa* Subzone in Djebel Zakamoune; ** Estimation of the duration of the lower Danian hiatus at Sidi Ziane based on the estimated age of the base of interval A_{D1} at Djebel Zakamoune.

Fig1

Click here to access/download;Figure;Fig1.tif

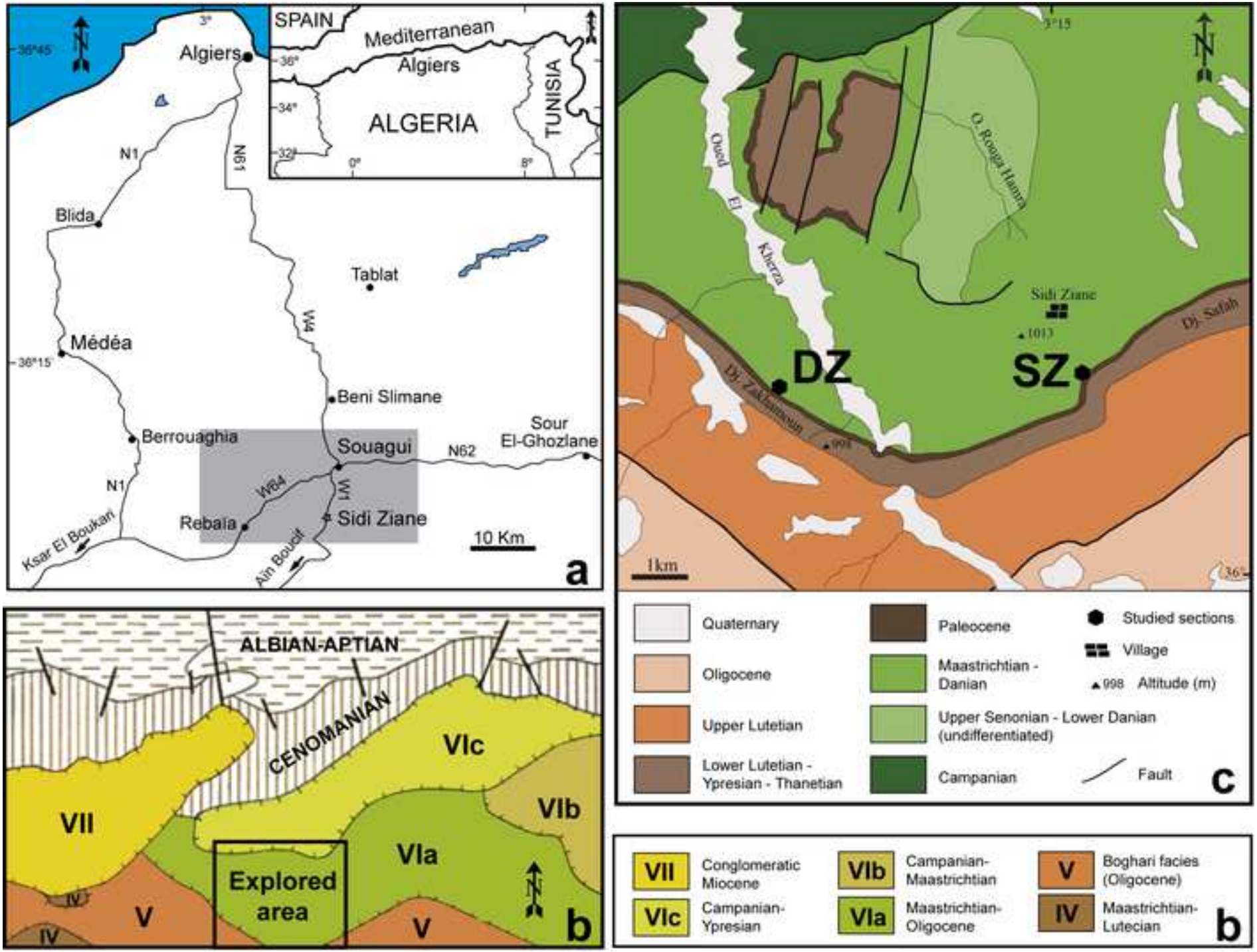

Fig2

Click here to access/download;Figure;Fig2.tif

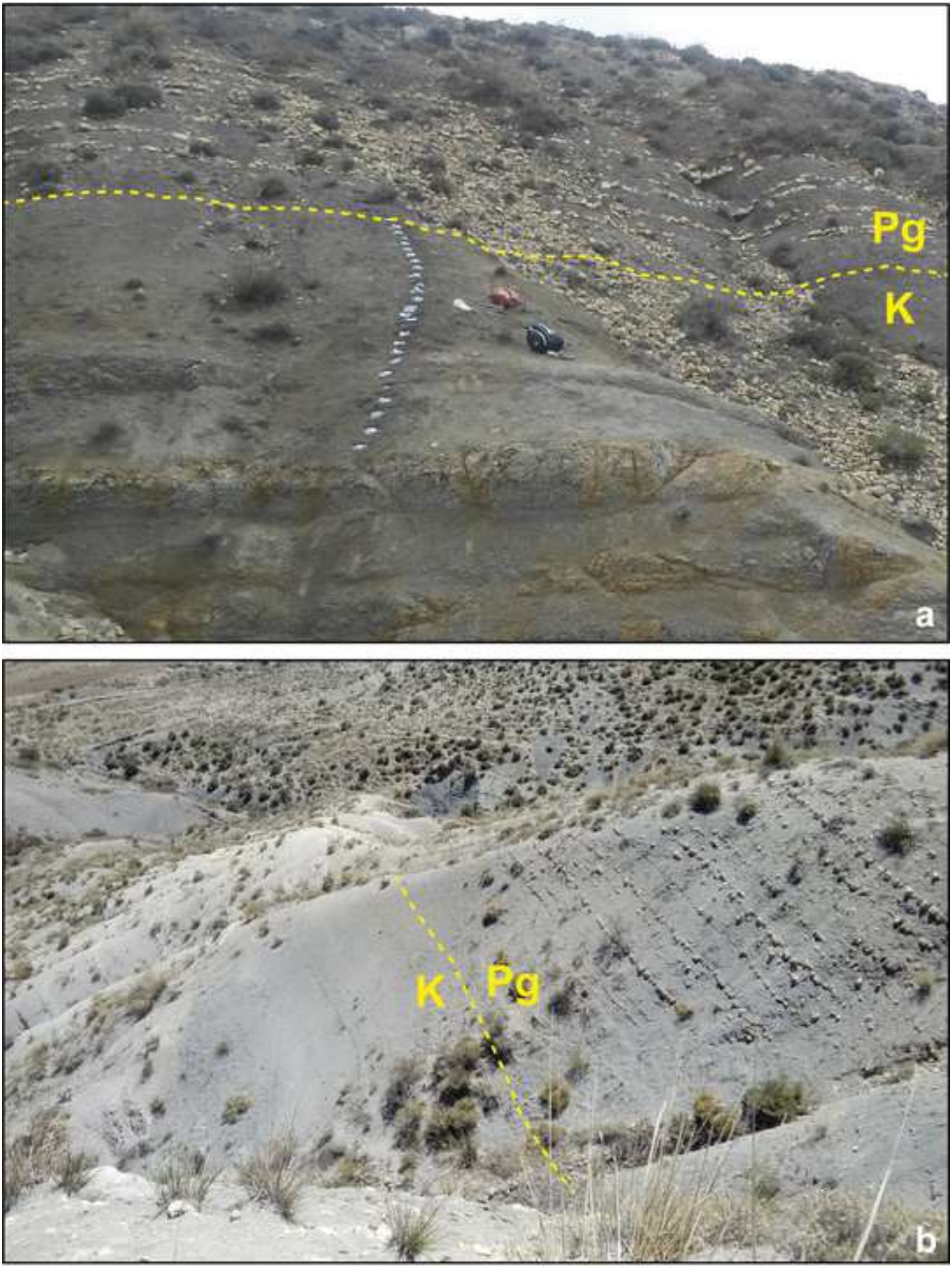

Fig3

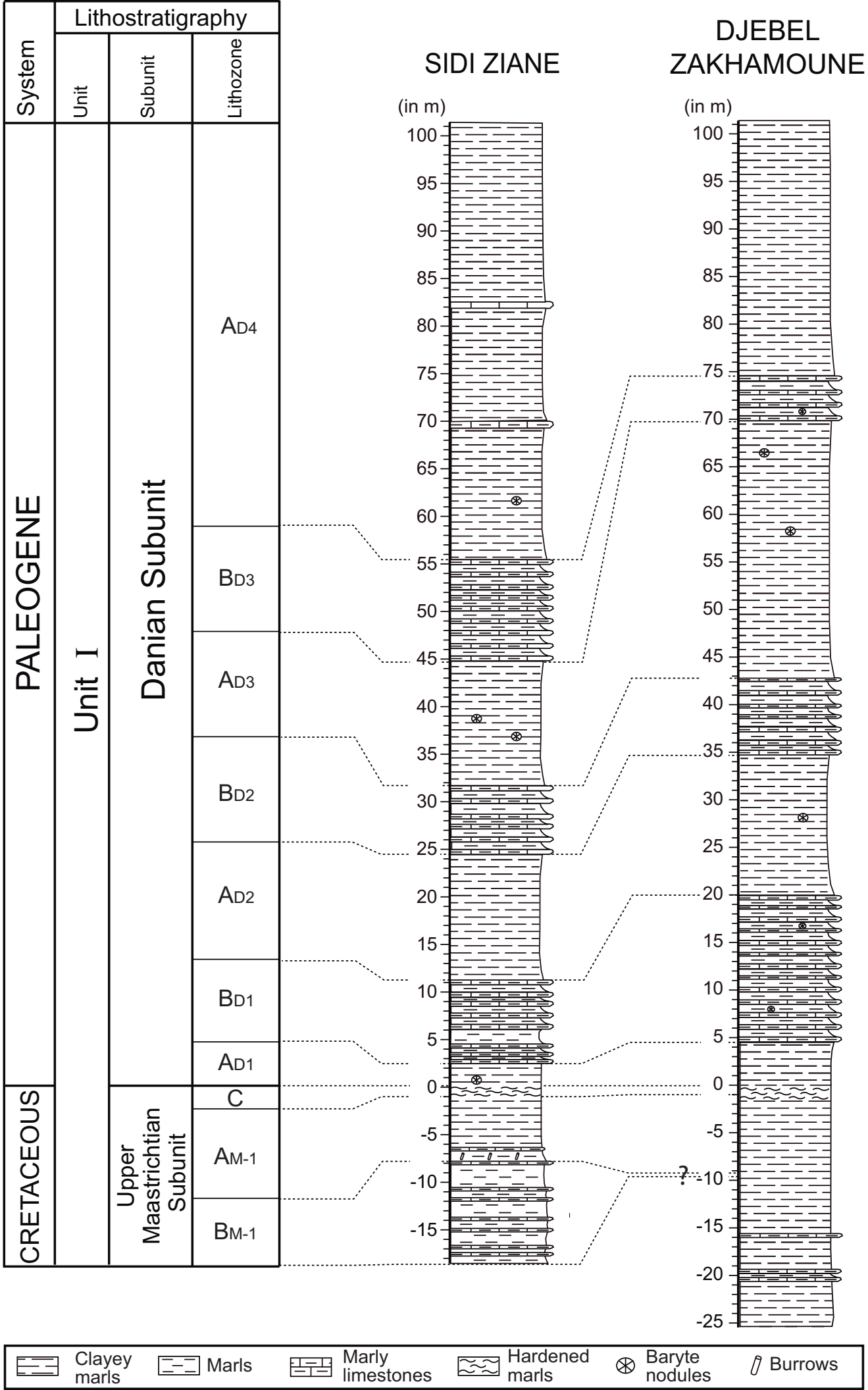
Lithostratigraphy
System
Unit
Subunit
Lithozone
PALEOGENE
Unit I
Danian Subunit
AD4
BD3
AD3
BD2
AD2
BD1
AD1
CRETACEOUS
Upper Maastrichtian Subunit
C
AM-1
BM-1
SIDI ZIANE
DJEBEL ZAKHAMOUNE
(in m)
100
95
90
85
80
75
70
65
60
55
50
45
40
35
30
25
20
15
10
5
0
-5
-10
-15
-20
-25
?
Clayey marls
Marls
Marly limestones
Hardened marls
Baryte nodules
Burrows

Fig4

Click here to access/download;Figure;Fig4.tif

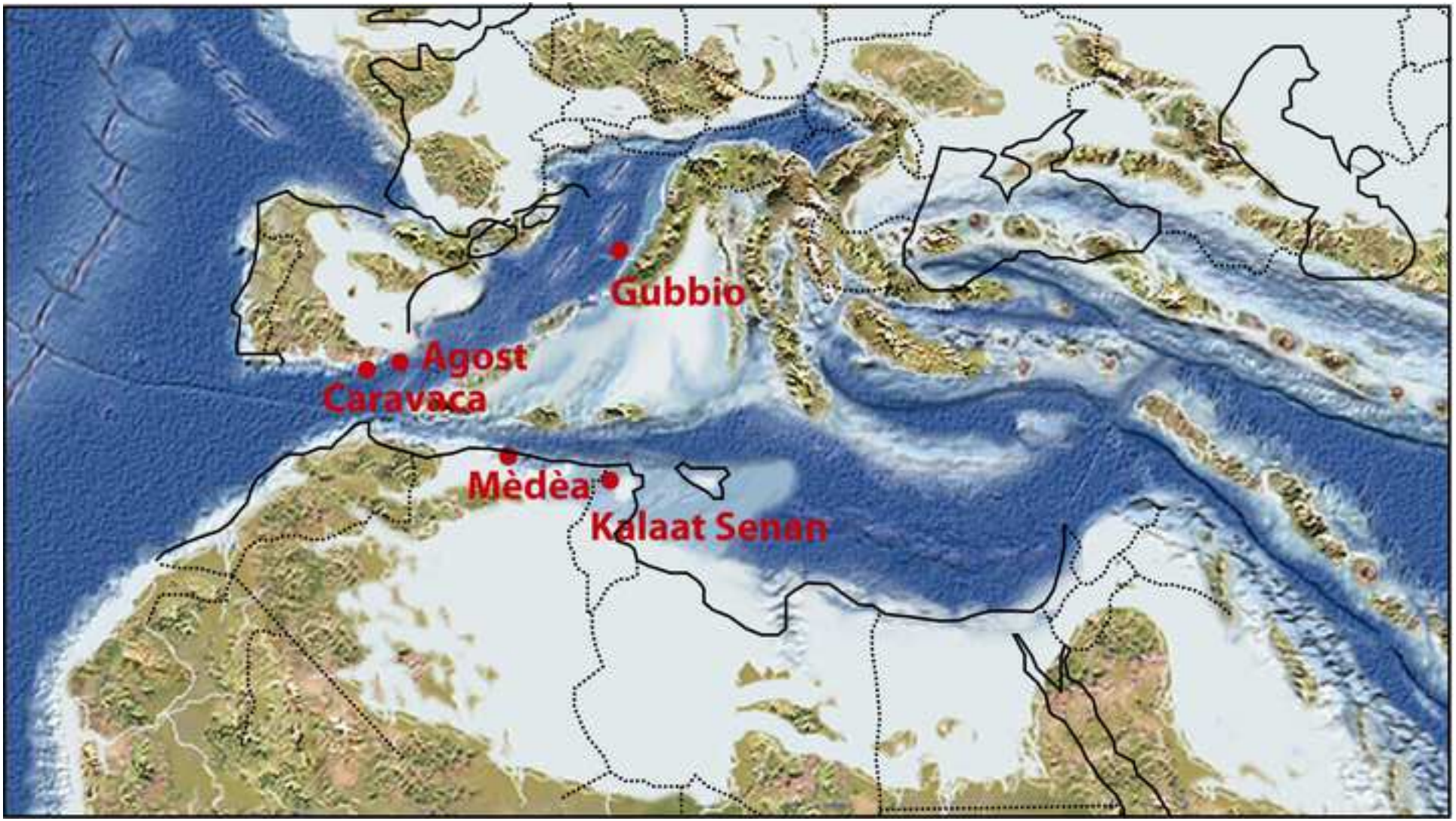

Fig5

UPPER MAASTRICHTIAN
DANIAN
Stages
C30n
C29r
C29n
C28r
C28n
C27r
C27n
C26r
Paleomagnetic reversal
-358
0
+352
+1082
+1373
+2546
+3523
+3819
Time since K/Pg boundary (kyrs)
Pseudoguembelina hariaensis
Plummerita hantkeninoides
Guembelitria cretacea
Parvularu-goglobigerina eugubina
Parasubbotina pseudobulloides
Acarinina trinidadensis
Acarinina uncinata
Hedbergella holmdelensis
Parvularu-goglobigerina longiapertura
Parvularu-goglobigerina sabina
Eoglobigerina simplicissima
Eoglobigerina trivialis
Subbotina triloculinoides
Globanomalina compressa
Biozones
(1)
(2)
(3)
(4)
CF3
CF2
CF1
M3
P0
Pα
P1a
P1b
P1c
P1d
P2
Gansserina gansseri
Archaeglobigerina cretacea
Abathomphalus mayaroensis
Plummerita hantkeninoides
Muricohedbergella holmdelensis
Guembelitria cretacea
Palaeoglobigerina alticonusa
Parvularugoglobigerina longiapertura
Parvularugoglobigerina sabina
Parvularugoglobigerina eugubina
Eoglobigerina simplicissima
Trochoguembelitria liuae
Praemurica taurica
Eoglobigerina cf. trivialis
Parasubbotina pseudobulloides
Praemurica inconstans
Subbotina triloculinoides
Globanomalina compressa
Acarinina trinidadensis
Globanomalina haunsbergensis
Acarinina uncinata
Luterbacheria ehrenbergi
Biochronostratigraphical ranges

Fig6

Click here to access/download;Figure;Fig6.tif

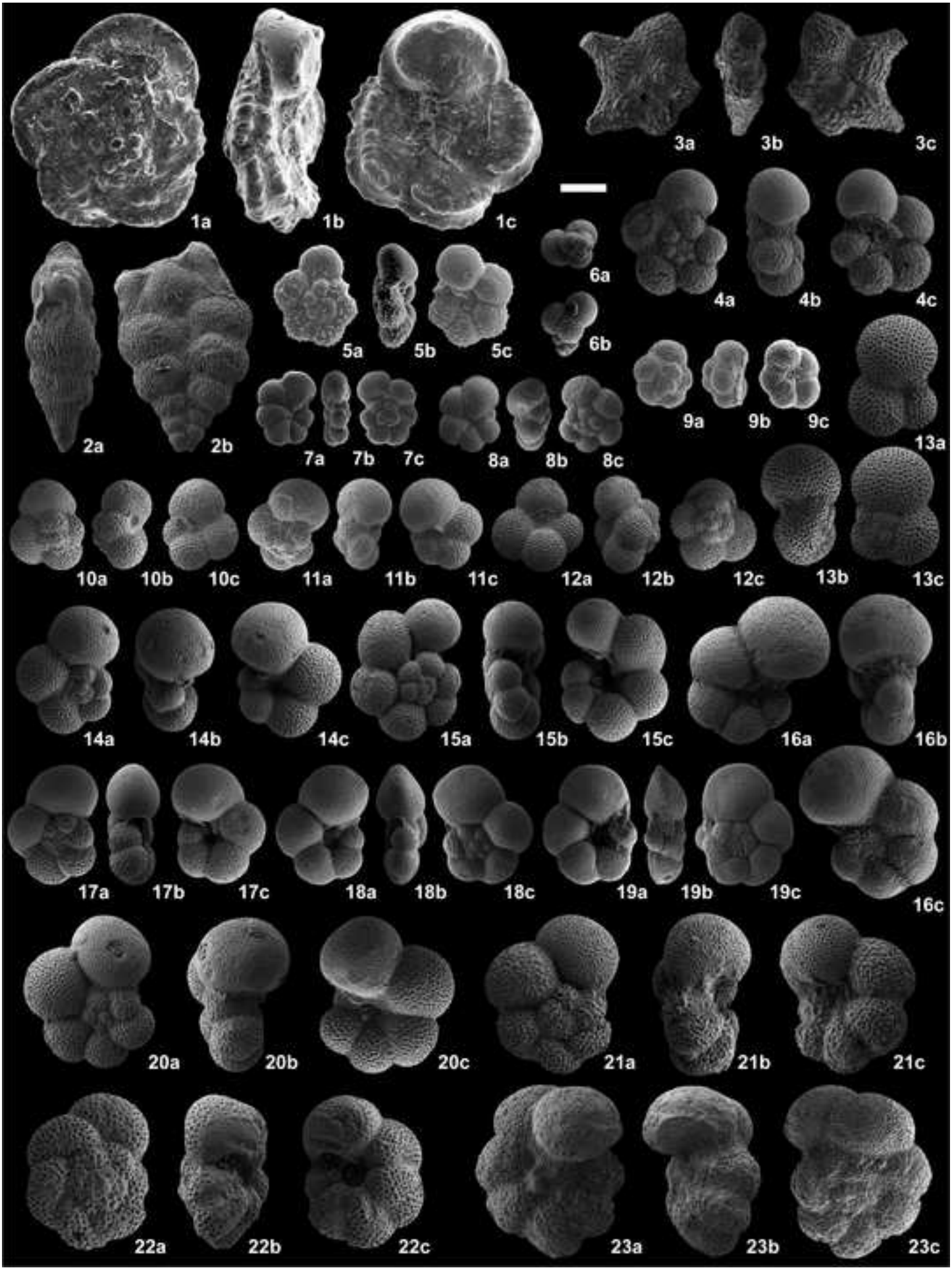

Fig7

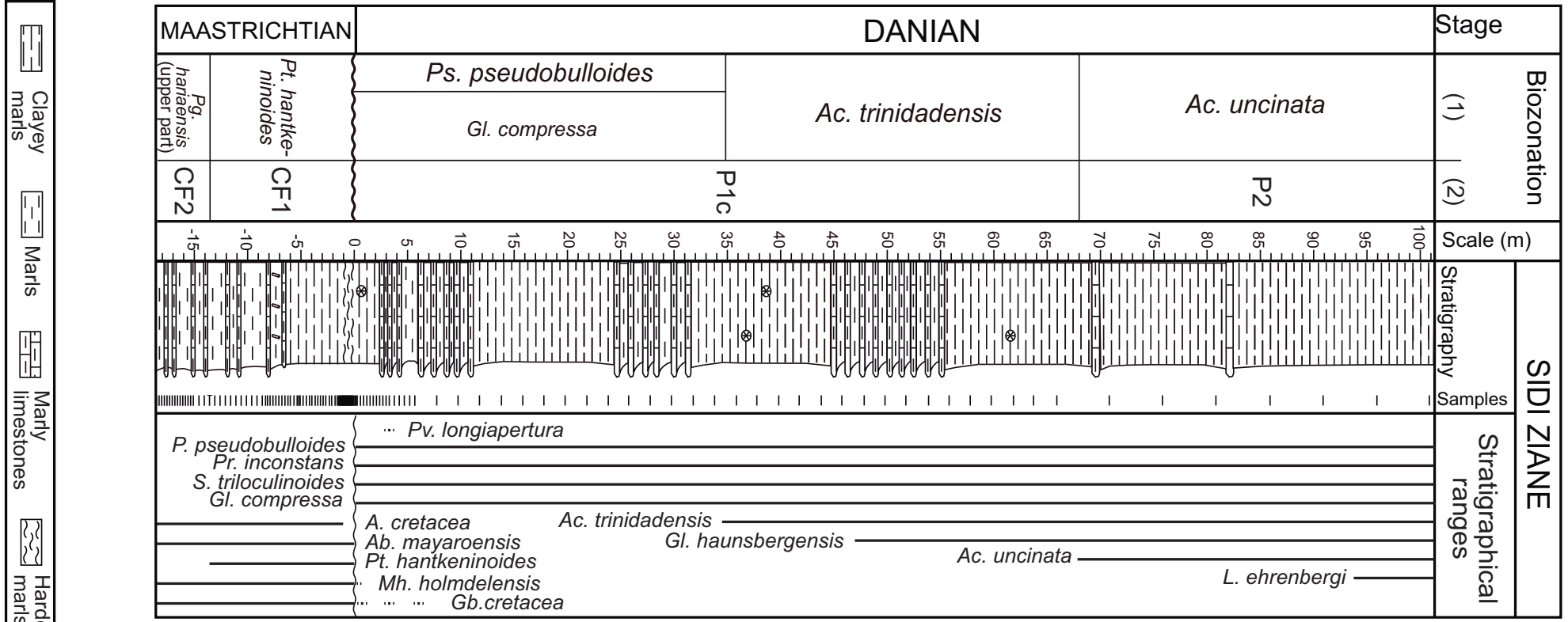

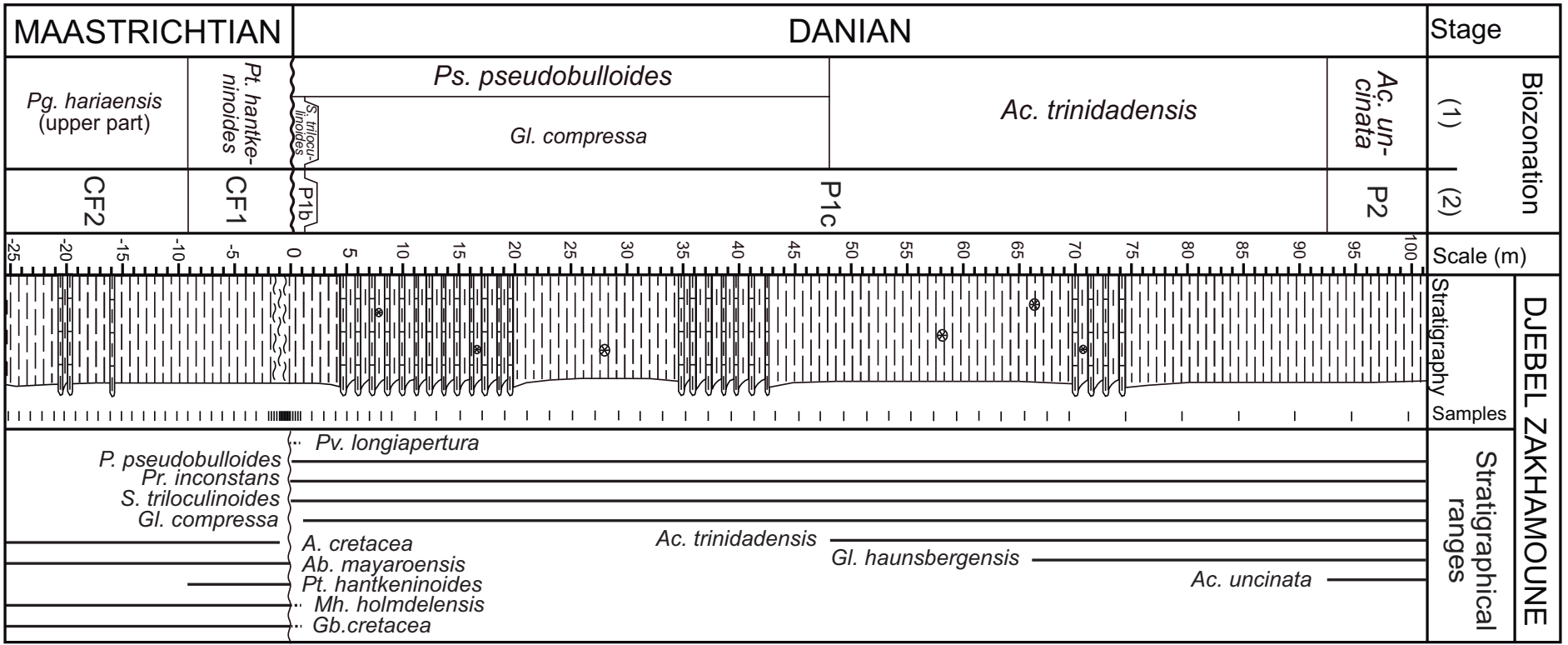

Clayey marls
Marls
Marly limestones
Hardened marls
Baryte nodules
Burrows
Reworked specimens

Fig8

Click here to access/download;Figure;Fig8.tif

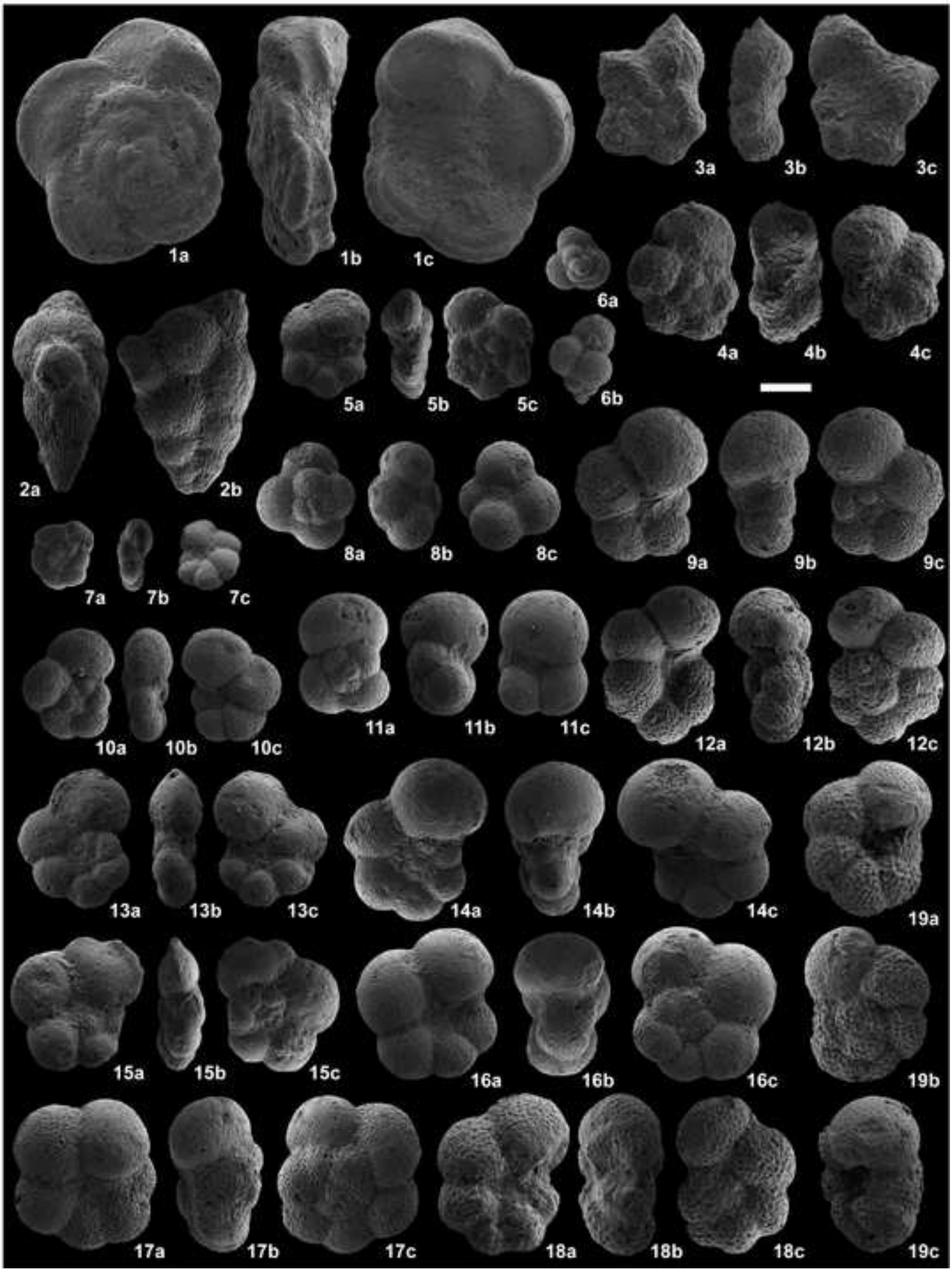

Fig9

Click here to access/download;Figure;Fig9.tif

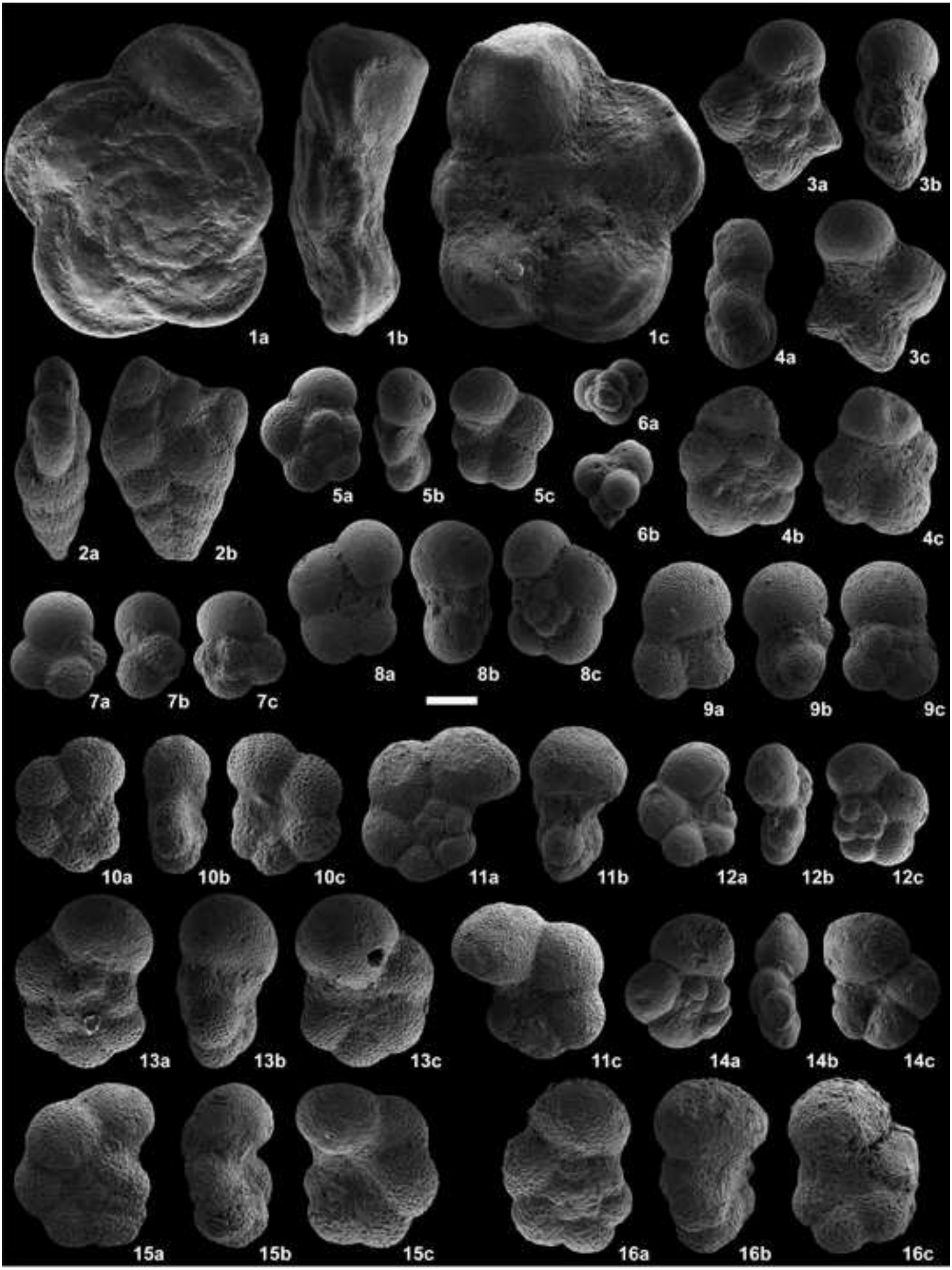

Fig10

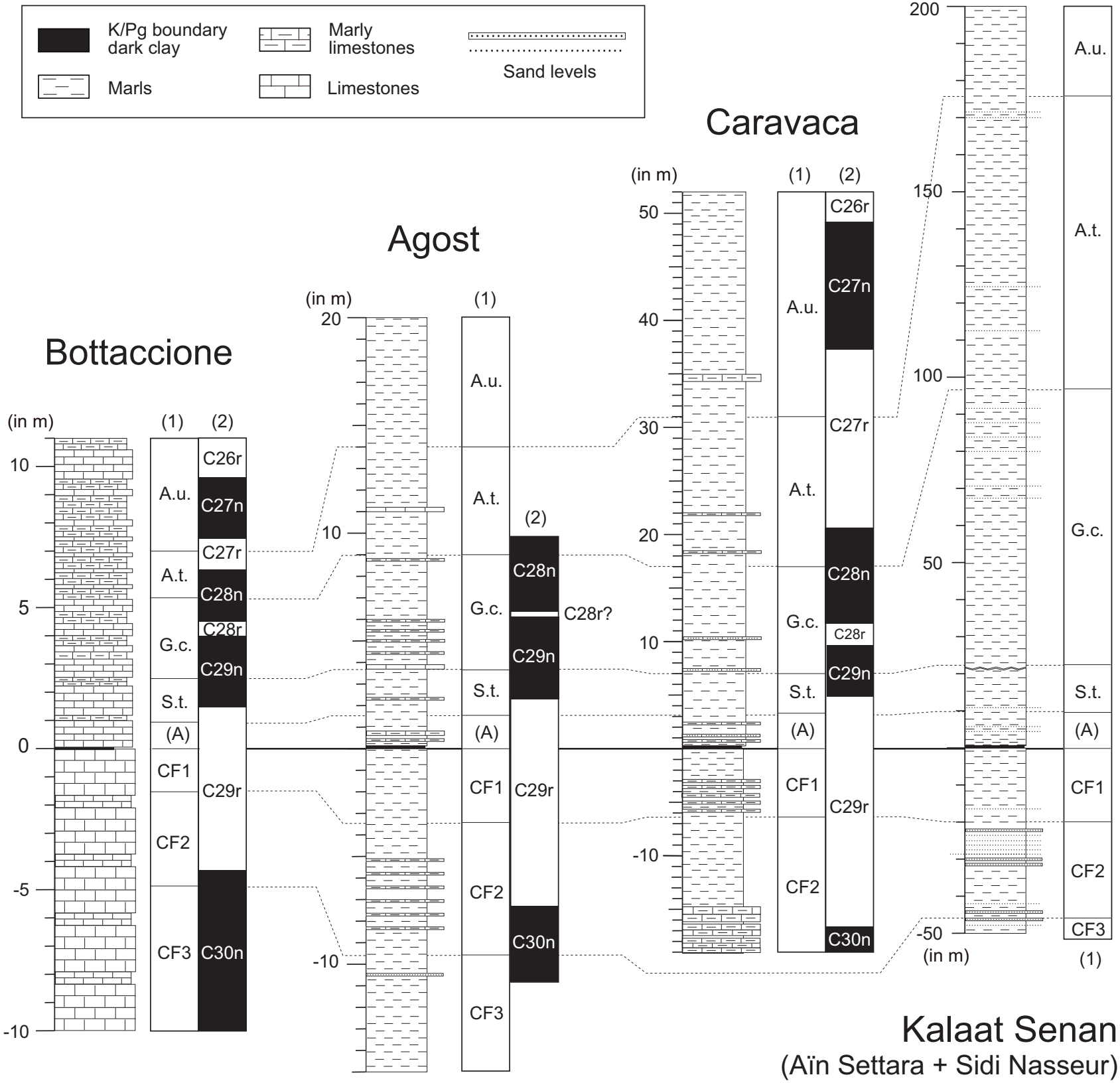
K/Pg boundary dark clay
Marly limestones
Sand levels
Marls
Limestones
Bottaccione
Agost
Caravaca
Kalaat Senan
(Aïn Settara + Sidi Nasseur)
(in m)
(1)
(2)
A.u.
A.t.
G.c.
S.t.
(A)
CF1
CF2
CF3
C26r
C27n
C27r
C28n
C28r
C28r?
C29n
C29r
C30n

Fig11

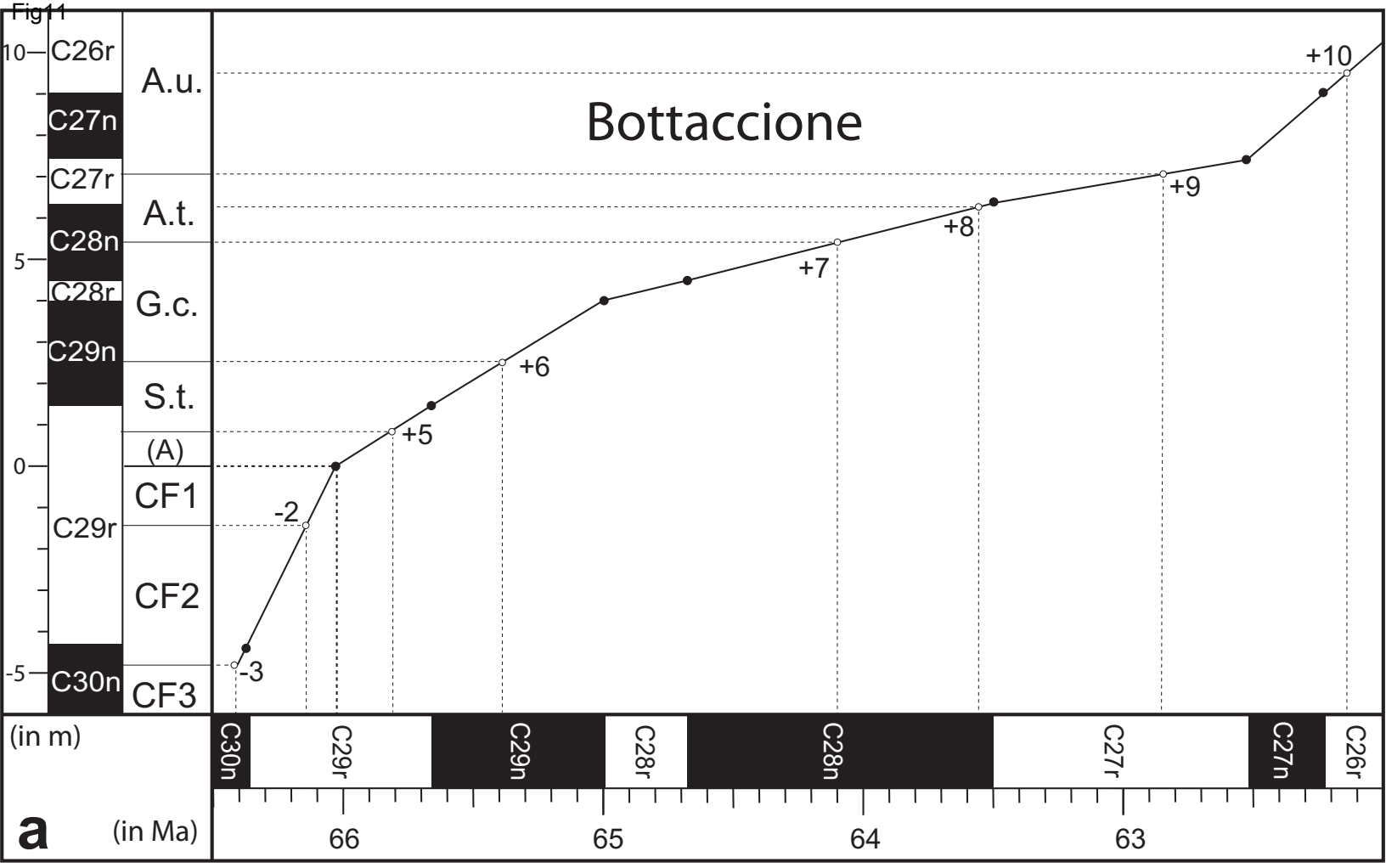
Bottaccione
C26r
C27n
C27r
C28n
C28r
C29n
C29r
C30n
A.u.
A.t.
G.c.
S.t.
(A)
CF1
CF2
CF3
10
5
0
-5
+10
+9
+8
+7
+6
+5
-2
-3
(in m)
C30n
C29r
C29n
C28r
C28n
C27r
C27n
C26r
66
65
64
63
(in Ma)

a

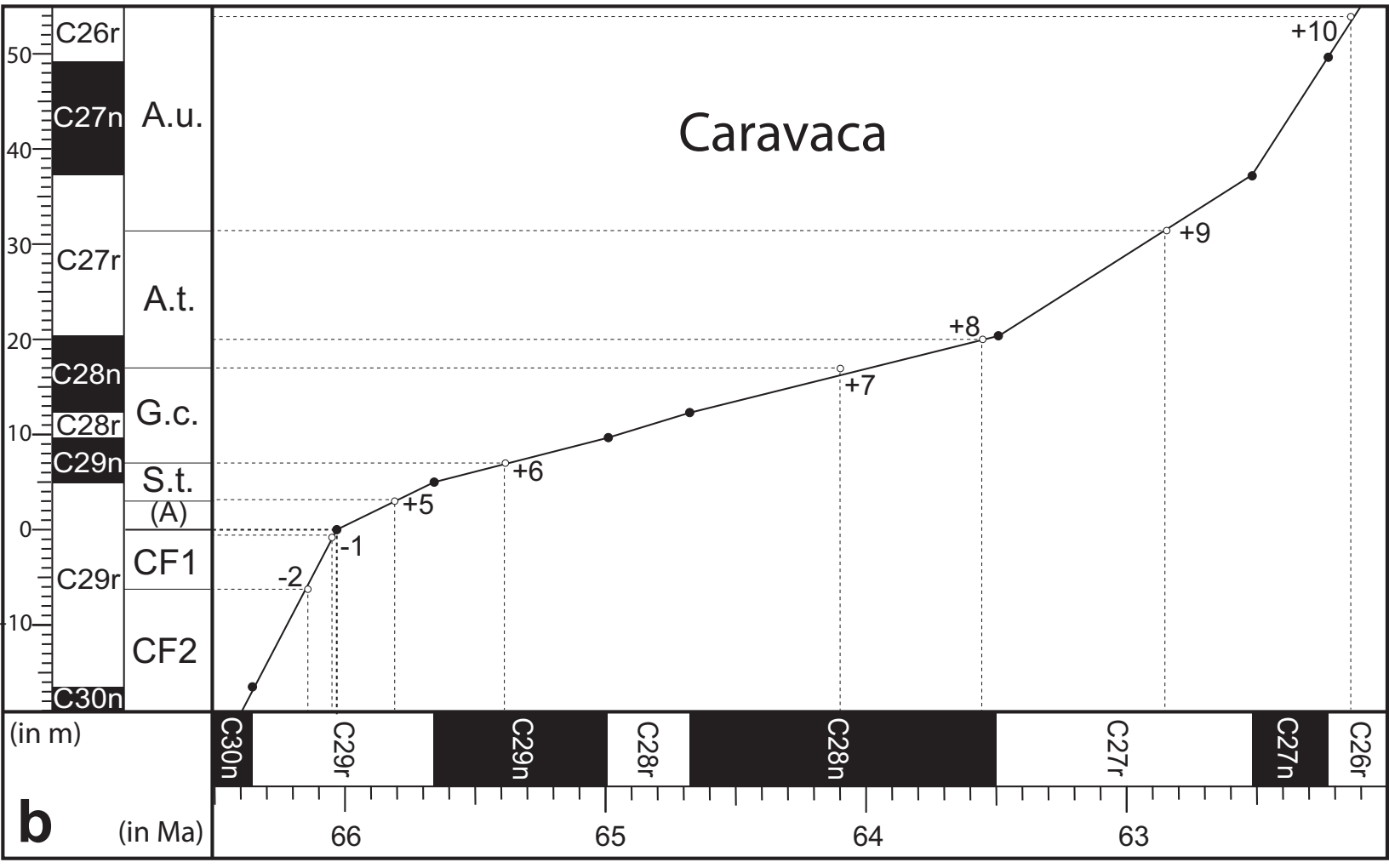
Caravaca
C26r
C27n
C27r
C28n
C28r
C29n
C29r
C30n
A.u.
A.t.
G.c.
S.t.
(A)
CF1
CF2
50
40
30
20
10
0
-10
+10
+9
+8
+7
+6
+5
-1
-2
(in m)
C30n
C29r
C29n
C28r
C28n
C27r
C27n
C26r
66
65
64
63
(in Ma)

b

Fig 12

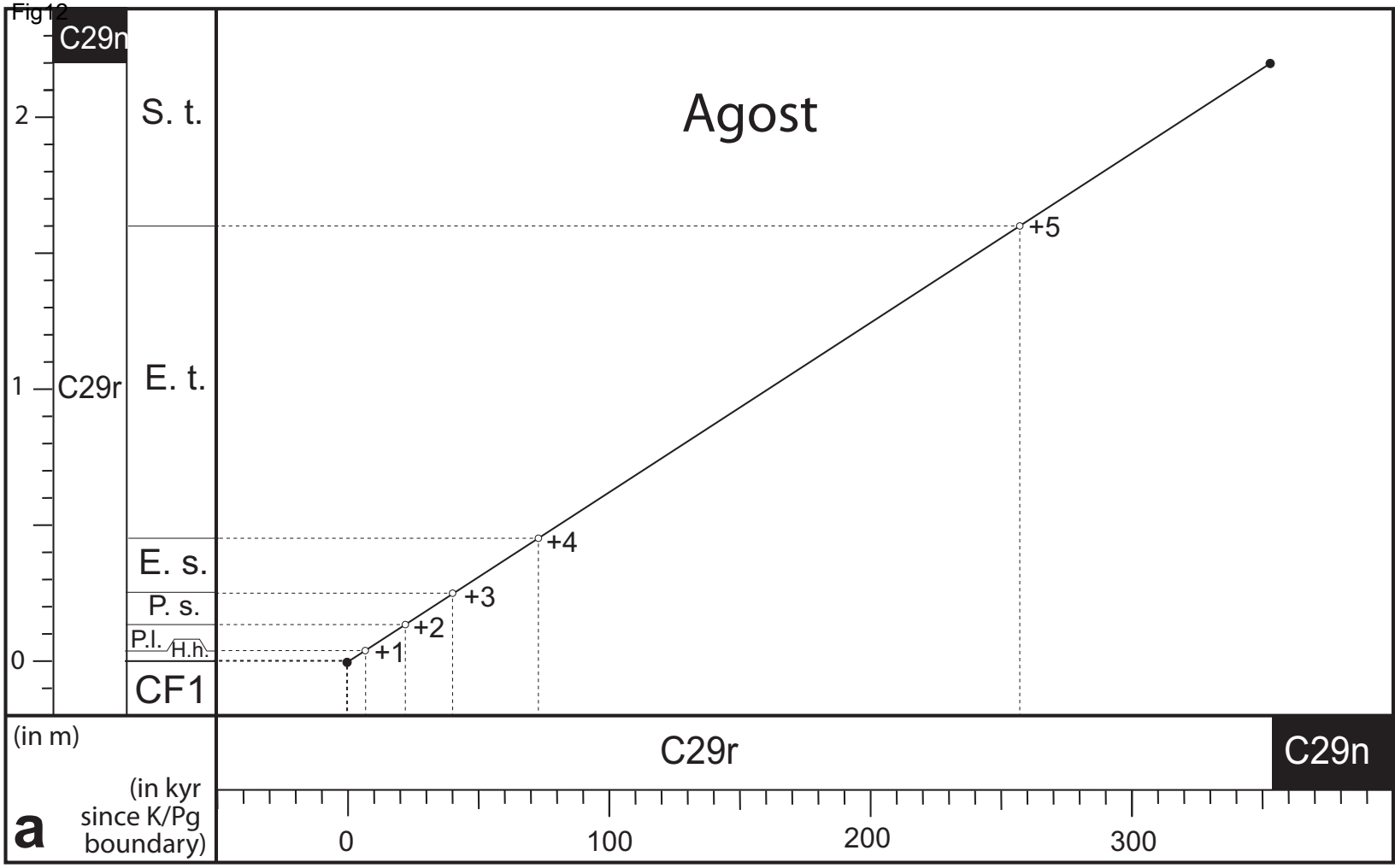
C29n
C29r
S. t.
E. t.
E. s.
P. s.
P.I.
H.h.
CF1
2
1
0
Agost
+1
+2
+3
+4
+5
(in m)
C29r
C29n
(in kyr since K/Pg boundary)
0
100
200
300
a

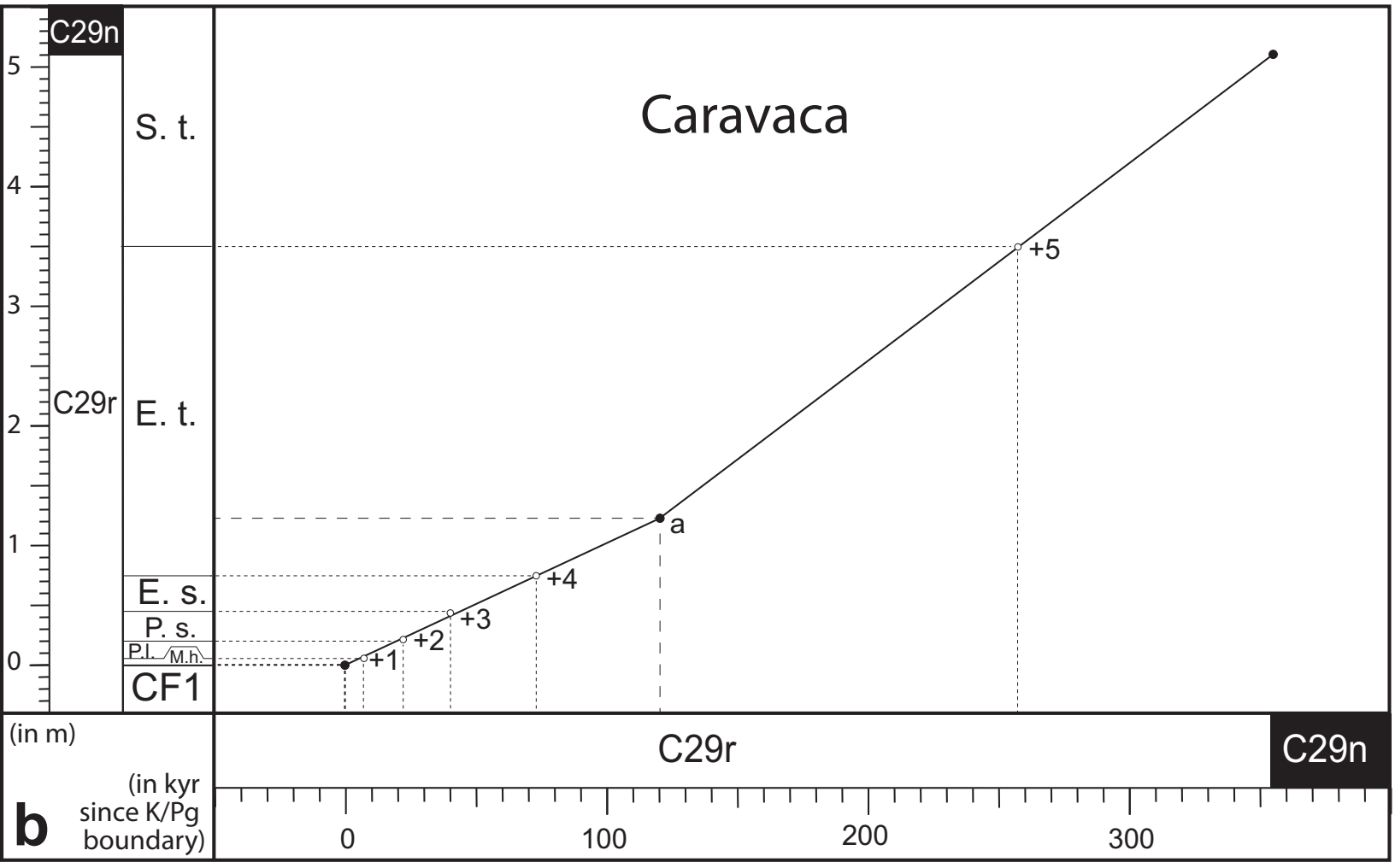
C29n
C29r
S. t.
E. t.
E. s.
P. s.
P.I.
M.h.
CF1
5
4
3
2
1
0
Caravaca
a
+1
+2
+3
+4
+5
(in m)
C29r
C29n
(in kyr since K/Pg boundary)
0
100
200
300
b

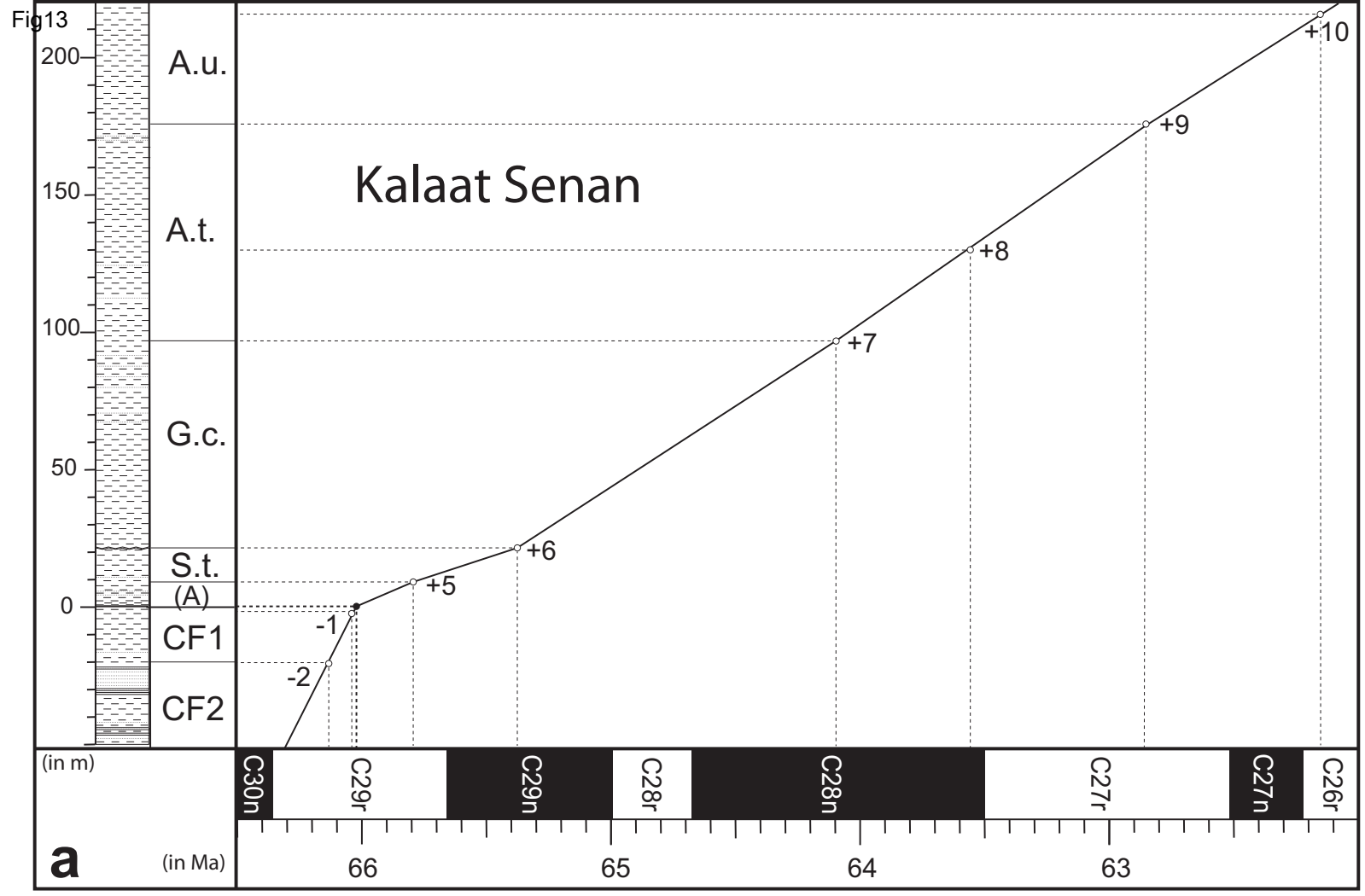
Fig13
Kalaat Senan
A.u.
A.t.
G.c.
S.t.
(A)
CF1
CF2
200
150
100
50
0
-2
-1
+5
+6
+7
+8
+9
+10
(in m)
C30n
C29r
C29n
C28r
C28n
C27r
C27n
C26r
66
65
64
63
(in Ma)
a

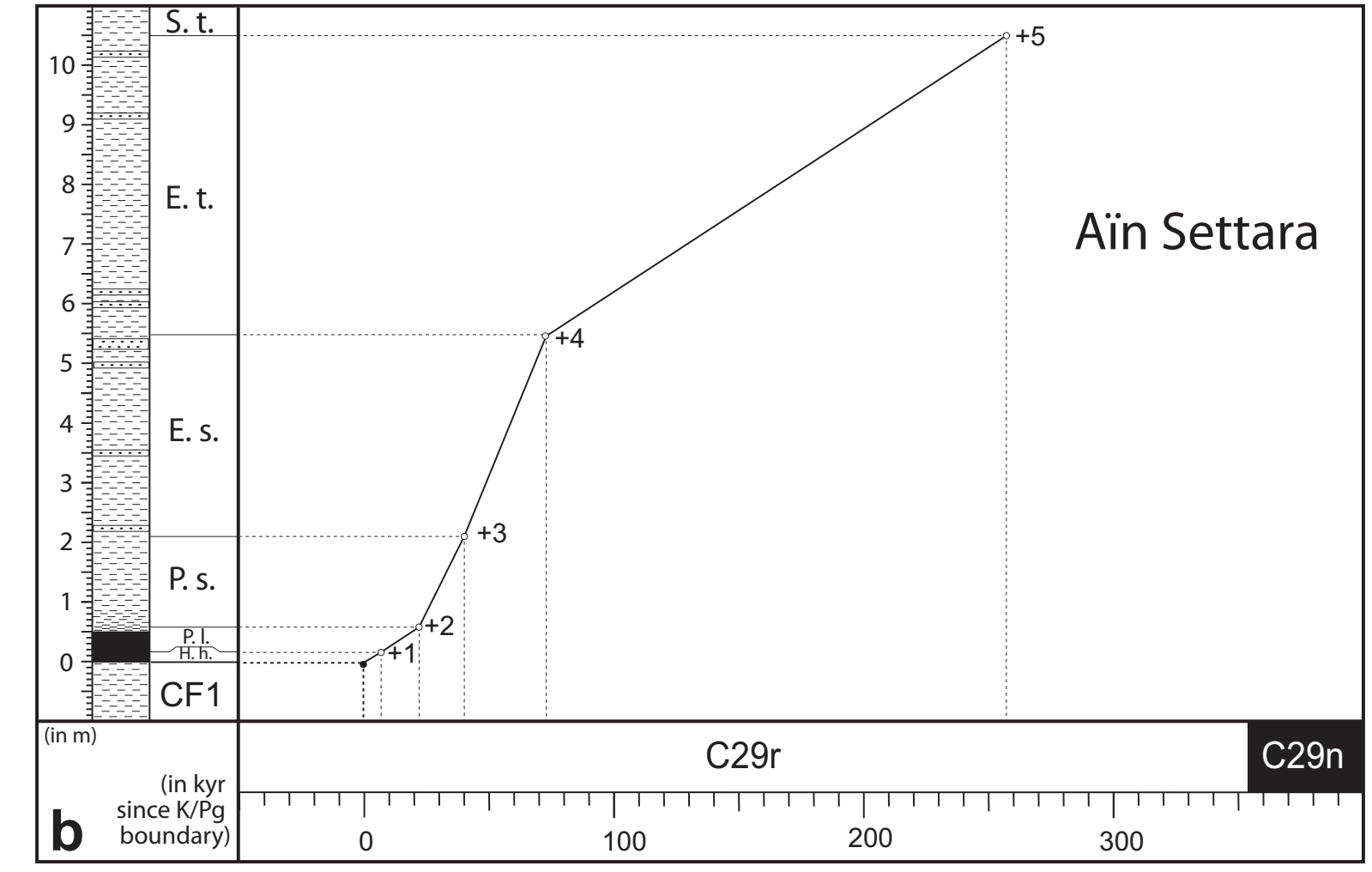
Aïn Settara
S. t.
E. t.
E. s.
P. s.
P. l.
H. h.
CF1
10
9
8
7
6
5
4
3
2
1
0
+1
+2
+3
+4
+5
(in m)
C29r
C29n
0
100
200
300
(in kyr since K/Pg boundary)
b

Fig14

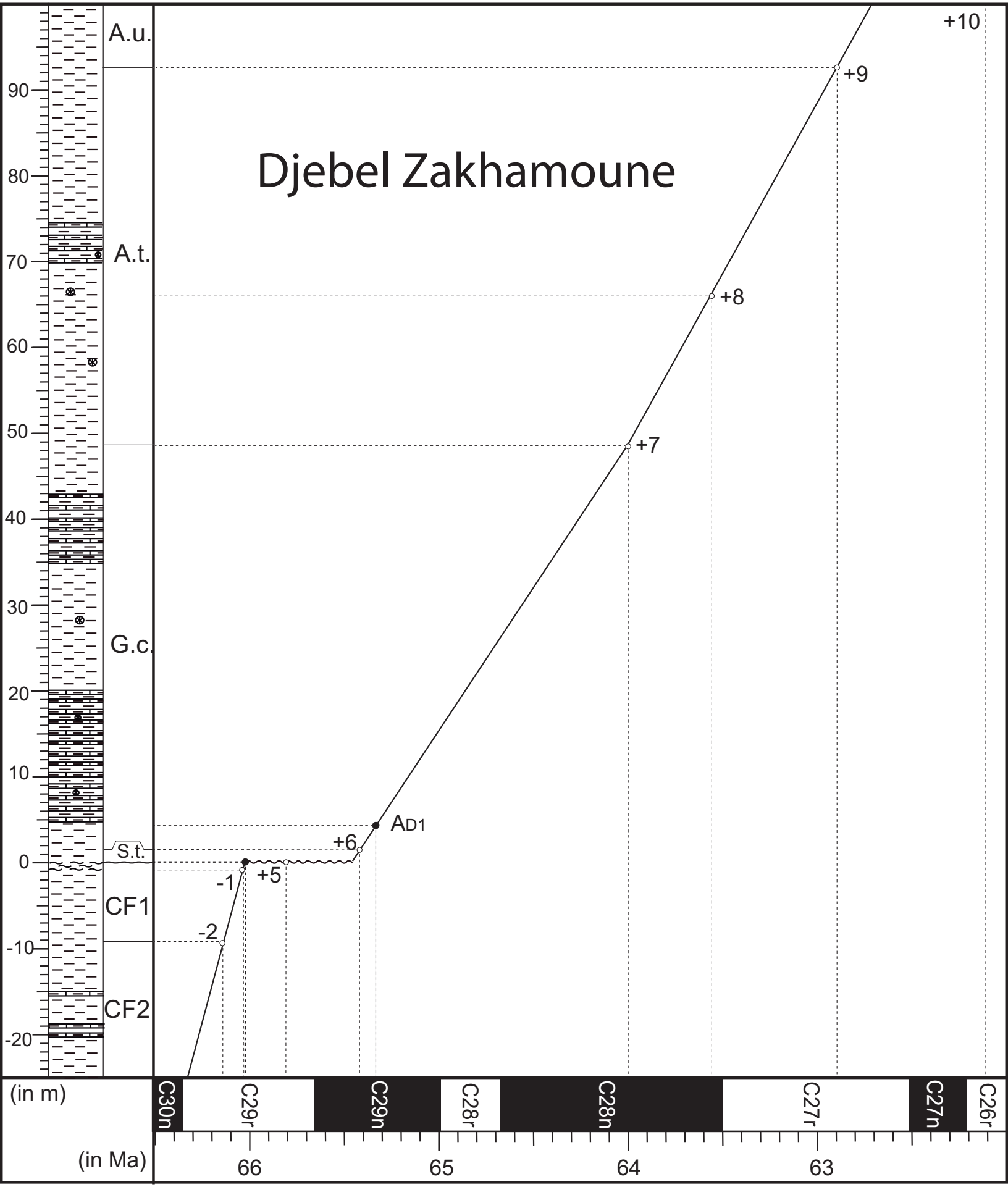
Djebel Zakhamoune
A.u.
A.t.
G.c.
S.t.
CF1
CF2
90
80
70
60
50
40
30
20
10
0
-10
-20
+10
+9
+8
+7
+6
+5
-1
-2
AD1
(in m)
(in Ma)
C30n
C29r
C29n
C28r
C28n
C27r
C27n
C26r
66
65
64
63

Fig15

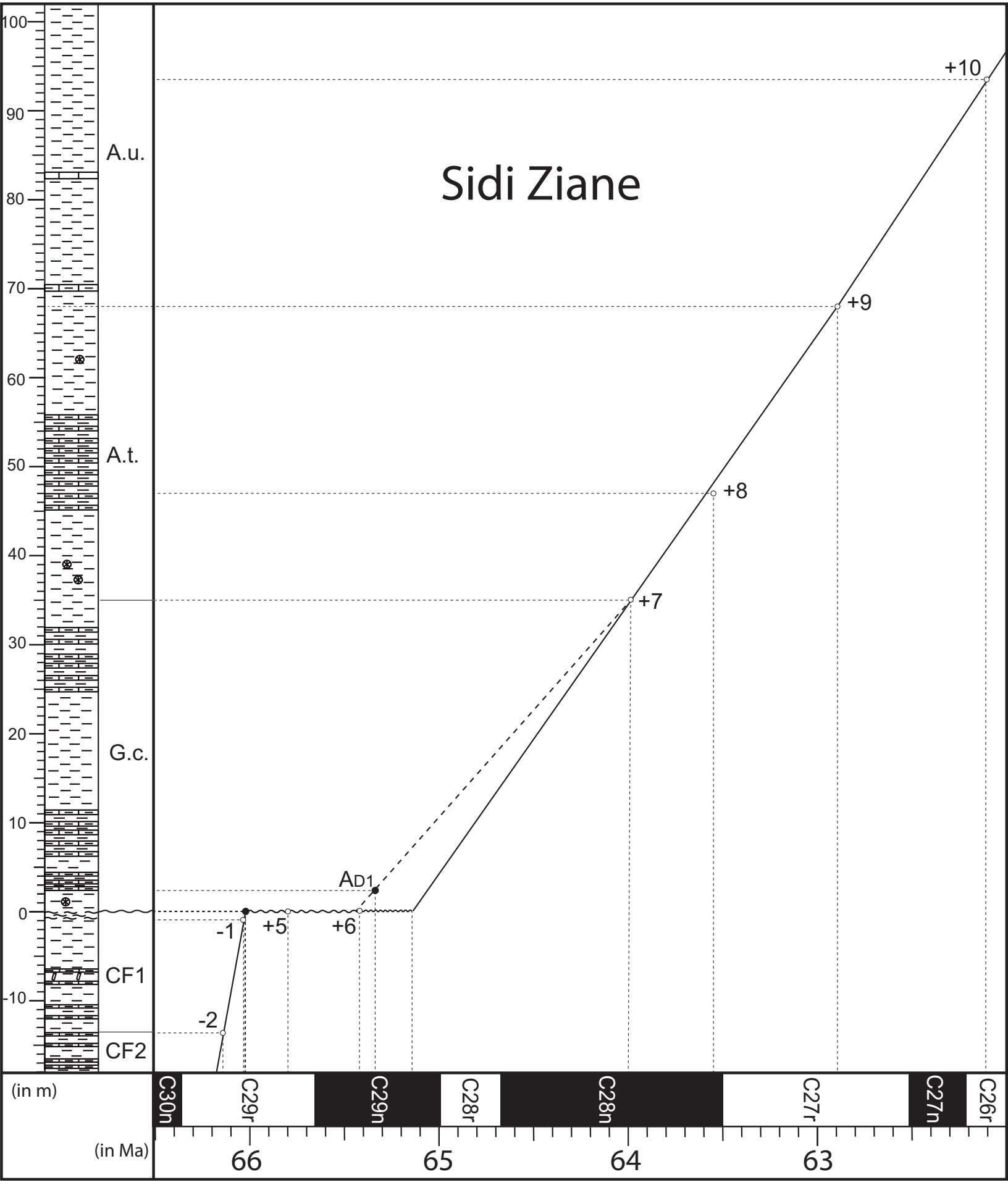
Sidi Ziane
100
90
80
70
60
50
40
30
20
10
0
-10
A.u.
A.t.
G.c.
CF1
CF2
+10
+9
+8
+7
+6
+5
-1
-2
AD1
(in m)
(in Ma)
C30n
C29r
C29n
C28r
C28n
C27r
C27n
C26r
66
65
64
63

Table1

BOTACCIONE (ITALY)					
	Boundary age (kyrs since K/Pg)	Magnetozone duration (kyrs)	Stratigraphic position (cm since K/Pg)	Magnetozone thickness (cm)	Sedimentation rate (cm/kyr)
C27n/C26r boundary	3819		900		
C27n		296		150	0.51
C27r/C27n boundary	3523		750		
C27r		977		120	0.12
C28n/C27r boundary	2546		630		
C28n		1173		180	0.15
C28r/C28n boundary	1373		450		
C28r		291		50	0.17
C29n/C28r boundary	1082		400		
C29n		730		250	0.34
C29r/C29n boundary	352		150		
upper C29r		352		150	0.43
K/Pg boundary	0		0		
lower C29r		358		427	1.19
C30n/C29r boundary	-358		-427		

AGOST (SPAIN)					
	Boundary age (kyrs since K/Pg)	Magnetozone duration (kyrs)	Stratigraphic position (cm since K/Pg)	Magnetozone thickness (cm)	Sedimentation rate (cm/kyr)
C29n/C28r boundary	1082		~ 600		
C29n		730		~ 380	0.52
C29r/C29n boundary	352		220		
upper C29r		352		220	0.62
K/Pg boundary	0		0		
lower C29r		358		750	2.09
C28n/C29r boundary	-358		-750		

CARAVACA (SPAIN)					
	Boundary age (kyrs since K/Pg)	Magnetozone duration (kyrs)	Stratigraphic position (cm since K/Pg)	Magnetozone thickness (cm)	Sedimentation rate (cm/kyr)
C27n/C26r boundary	3819		4920		
C27n		296		1190	4.02
C27r/C27n boundary	3523		3730		
C27r		977		1700	1.74
C28n/C27r boundary	2546		2030		
C28n		1173		800	0.68
C28r/C28n boundary	1373		1230		
C28r		291		250	0.86
C29n/C28r boundary	1082		980		
C29n		730		470	0.64
C29r/C29n boundary	352		510		
upper C29r ↑		230		388	1.67
Change in sedimentation rate *	122		120		
upper C29r ↓		122		122	1.02
K/Pg boundary	0		0		
lower C29r		358		1650	4.61
C28n/C29r boundary	-358		-1650		

Datum	BOTACCIONE (ITALY)		AGOST (SPAIN)		CARAVACA (SPAIN)		Average age (kyr)	Average age (Ma)
	Stratigraphic position (cm)	Bioevent age (kyr)	Stratigraphic position (cm)	Bioevent age (kyr)	Stratigraphic position (cm)	Bioevent age (kyr)		
LOD/FA L. ehrenbergi	960	3937.4	-	-	5400	3938.4	3937.9	62.102
LOD/FA Ac. uncinata	700	3115.9	-	-	3100	3160.9	3138.4	62.902
LOD/FA G. haunsbergensis	620	2480.8	-	-	2000	2502.0	2491,4	63.549
LOD/FA Ac. trinidadensis	550	2024.7	-	-	1700	2062.1	2043.4	63.997
LOD/FA G. compressa	240	614.8	380	659.1	700	647.1	640.3	65.400
LOD/FA S. triloculinoides	-	-	160	256.0	380	240.2	248.1	65.792
LOD/FA P. pseudobulloides	-	-	45	72.0	77	75.7	73.8	65.966
LOD E. simplicissima	-	-	26	41.6	45	44.2	42.9	65.997
LOD Pv. eugubina	-	-	14	22.4	18	19.7	21.0	66.019
LOD Pv. longiapertura	-	-	4	6.4	5	4.9	5.6	66.034
K/Pg boundary	0	0	0	0	0	0	0	66.040
HOD/LA A. cretacea	-	-	-30	-14.3	-50	-10.8	-12.6	66.053
LOD/FA Pt. hantkeninoides	-140	-117.1	-345	-164.7	-630	-136.7	-139.6	66.191
HOD/LA Gs. gansseri	-480	-402.4	-950	-453.5	-	-	-428.0	66.468

Table2

KALAAT SENAN (TUNISIA): AÏN SETTARA + SIDI NASSEUR				
Datum/Biozone	Estimated age (kyr)	Stratigraphic position (cm since K/Pg)	Biozone thickness (cm)	Sedimentation rate (cm/kyr)
LOD/FA *L. ehrenbergi*	3937.9	21500		
LOD/FA *Ac. uncinata*	3138.4	17500		
LOD/FA *G. haunsbergensis*	2491.4	13000		
***Ac. trinidadensis* Zone**			7800	7. 12
LOD/FA *Ac. trinidadensis*	2043.4	9700		
***G. compressa* Subzone**			7500	5.34
LOD/FA *G. compressa*	640.3	2200		
***S. triloculinoides* Subzone**			1150	2.93
LOD/FA *S. triloculinoides*	248.1	1050		
***E. trivialis* Subzone**			500	2.87
LOD/FA *P. pseudobulloides*	73.8	550		
***E. simplicissima* Subzone**			340	11.00
LOD/FA *E. simplicissima*	42.9	210		
***Pv. sabina* Subzone**			150	6.85
LOD/FA *Pv. eugubina*	21.0	60		
***Pv. longiapertura* Subzone**			45	2.92
LOD/FA *Pv. longiapertura*	5.6	15		
***Mg. hedbergella* Subzone**			15	2.68
K/Pg boundary	0	0		
HOD/LA *A. cretacea*	-12.6	-140		
Zone CF1			1950	14.25
LOD/FA *Pt. hantkeninoides*	-139.6	-1950		
Zone CF2			2650	9.19
HOD/LA *Gs. gansseri*	-428.0	-4600		

Table3

DJEBEL ZAKHAMOUNE				
Datum/Biozone	Estimated age (kyr)	Stratigraphic position (cm from the K/Pg boundary)	Biozone thickness (cm)	Sedimentation rate (cm/kyr)
LOD/FA *L. ehrenbergi*	3937.9			
LOD/FA *Ac. uncinata*	3138.4	9250		
LOD/FA *G. haunsbergensis*	2491.4	6600		
***Ac. trinidadensis* Zone**			4300	4.06
LOD/FA *Ac. trinidadensis*	2043.4	4800		
Base of interval A_{D1}	744.8*	450		
***G. compressa* Subzone**			280	3.35
LOD/FA *G. compressa*	640.3	100		
Estimated duration for the lower Danian hiatus = 610.4 kyr				
***S. triloculinoides* Subzone**			-	-
LOD/FA *S. triloculinoides*	248.1	0		
***E. trivialis* Subzone**			-	-
LOD/FA *P. pseudobulloides*	73.8	0		
***E. simplicissima* Subzone**			-	-
LOD/FA *E. simplicissima*	42.9	-		
***Pv. sabina* Subzone**			-	-
LOD/FA *Pv. eugubina*	21.0	-		
***Pv. longiapertura* Subzone**			-	-
LOD/FA *Pv. longiapertura*	5.6	-		
***Mg. hedbergella* Subzone**			-	-
K/Pg boundary	0	0		
HOD/LA *A. cretacea*	-12.6	-100		
Zone CF1			900	6.58
LOD/FA *Pt. hantkeninoides*	-139.6	-900		

SIDI ZIANE				
Datum/Biozone	Estimated age (kyr)	Stratigraphic position (cm from the K/Pg boundary)	Biozone thickness (cm)	Sedimentation rate (cm/kyr)
LOD/FA *L. ehrenbergi*	3937.9	9400		
LOD/FA *Ac. uncinata*	3138.4	6800		
LOD/FA *G. haunsbergensis*	2491,4	4700		
Ac. trinidadensis Zone			1200	3.01
LOD/FA Ac. trinidadensis	2043.4	3500		
Base of interval A_{D1}	744.8*	250	250**	2.50**
Estimated duration for the lower Danian hiatus** = 644.9 kyr				
***G. compressa* Subzone**			-	-
LOD/FA G. compressa	640.3	0		
***S. triloculinoides* Subzone**			-	-
LOD/FA *S. triloculinoides*	248.1	0		
***E. trivialis* Subzone**			-	-
LOD/FA *P. pseudobulloides*	73.8	0		
***E. simplicissima* Subzone**			-	-
LOD/FA *E. simplicissima*	42.9	-		
***Pv. sabina* Subzone**			-	-
LOD/FA *Pv. eugubina*	21.0	-		
***Pv. longiapertura* Subzone**			-	-
LOD/FA *Pv. longiapertura*	5.6	-		
***Mg. hedbergella* Subzone**			-	-
K/Pg boundary	0	0		
HOD/LA *A. cretacea*	-12.6	-120		
Zone CF1			1350	8.98
LOD/FA *Pt. hantkeninoides*	-139.6	-1350		